

Addis Ababa University

Addis Ababa Institute of Technology

School of Civil and Environmental Engineering



**MSc Thesis on Development of Intensity Duration Frequency (IDF) Curves
for Merawi Town, Ethiopia, Using Stationary Approach Submitted to the
School of Postgraduate Studies in Partial Fulfillment of the Requirements for
the Degree of Master of Science in Civil and Environmental (Hydraulic)
Engineering at Addis Ababa University**

Advisor:

Yenesew Mengiste (PHD)

Prepared and Submitted by

Tebikew Dereje Alemu

Addis Ababa, Ethiopia

June: 2024

CERTIFICATION

Undoubtedly, I would like to state that the thesis work titled "Development of Intensity Duration Frequency (IDF) Curves for Merawi Town, Ethiopia, Using Stationary Approach" is my own work. This thesis work submitted to the school of postgraduate studies at Addis Ababa Institute of Technology, Addis Ababa University, Ethiopia in partial fulfillment of the requirements for Award of Master of Science (MSc) degree in civil (hydraulic) engineering. I would like to verify that this thesis work has not been published by other professionals or graduates in order to be approved for the award of any other degree from another university, provided that the notes from the publications have been properly cited or acknowledged.

Prepared and Submitted By

Tebikew Dereje Alemu

Approval by Board of Examiners

Advisor

Yenesew Mengiste (PHD)

Signature



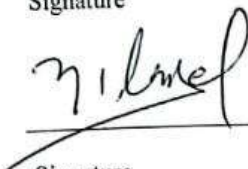
Date

20 June 2024

Internal Examiner

Yilma Seleshi (Professor)

Signature



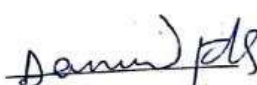
Date

19/6/24

External Examiner

Daneal Fekersillassie (PHD)

Signature



Date

19/6/24

Date

Chairman (Department of Graduate Committee)



Abraham Gebre (Dr.)
Dean, School of Civil &
Environmental Engineering



ABSTRACT

Planning and management of water resources depend heavily on intensity duration frequency curves because they show the statistical relationship between rainfall frequency and intensity duration. This thesis used the universal extreme value stationary approach, which is implemented in the R statistical programming environment, to give a thorough examination into the development of rainfall intensity duration frequency curves. The study starts out by going over the theoretical understanding of the general extreme value model and how it is applied to the process of creating rainfall intensity duration frequency curves. Next, using specific packages and functions to effectively handle rainfall data, fit the general extreme value distribution, and produce the final intensity duration frequency curves; it explores the step-by-step implementation of the general extreme value stationary approach in R studio. For the duration of the observation periods, the stationary model takes constant parameters into consideration. Estimating the distribution parameters involved applying the maximum likelihood estimator method. Statistical programming software R-studio was utilized to compute the distribution parameters, intensity levels, and fit the GEV stationary model to sample rainfall data. For four neighboring rainfall sites, the National Meteorological Agency in Addis Ababa, Ethiopia, provided the necessary historical rainfall data. Various tests and trends using the rainfall data were looked at. The Man-Kendall trend test at each station's rainfall data showed no patterns. The stationary model was adopted for return levels estimation for all rainfall stations instead of the non-stationary model due to the lack of trend results. The distribution parameters of the parameter model were used to forecast the return levels for each return term of 2, 5, 10, 25, 50, and 100 years. Since the model did not exhibit time-varying variability, it was possible to derive maximum return level outputs directly from the general extreme value fitted to the maximum annual rainfall. The return levels were then plotted on the x-y axis and translated to rainfall intensity using a simple formula. In practice, longer return periods yielded higher values than shorter return periods when computing rainfall intensity. For instance, a 15-minute rainstorm stationary model with a 25-year return period produced an intensity of 178.28 mm/hr, while a 15-minute rainstorm with a 100-year return period produced 261.2 mm/hr of rainfall.

Keywords: Stationary Model, Quantile Plot, R-studio, Merawi Town, Diagnostic Test

ACKNOWLEDGMENT

I want to thank Yenesew Mengiste (PHD), my advisor, first and foremost, for her unwavering support and direction. This study has been greatly influenced by her commitment, knowledge, and shrewd criticism. She has spent innumerable hours mentoring me through her academic journey, and I am appreciative of her support and patience. Her counsel and insight have been a real source of motivation.

I would like to thank my mother, Asmarech Abe Esteziaw, for her everlasting love, support, and faith in my skills. She has been a continual source of strength and energy for me while I have worked on my thesis. Her sacrifices, moral support, and awareness have been priceless. I consider myself really fortunate to have a mother like her; she has always encouraged me and supported me in whatever way she could, and I am appreciative of that.

Iyuel Girma and Alemayehu Mamo, my classmates, are also acknowledged for their invaluable contributions to this endeavor, along with those of my mother and advisor. Their support, wisdom, and encouragement have greatly influenced the direction this thesis has taken. This job has been completed successfully in large part because of their contributions.

I also like to thank Wolkite University and the Ministry of Education, the financing institutions, for their financial support. Their financial help has enabled me to continue my work and has played a part in making it a reality.

In conclusion, I express my gratitude to all of my friends, family, and coworkers for their unwavering support throughout this journey. I have always found inspiration and energy in their words of support, understanding, and encouragement.

TABLE OF CONTENTS

CERTIFICATION	Error! Bookmark not defined.
ABSTRACT.....	II
TABLE OF CONTENTS.....	V
LIST OF TABLES.....	VIII
LIST OF FIGURES	IX
LIST OF ABBREVIATIONS.....	X
CHAPTER 1: INTRODUCTION	1
1.1 Background.....	1
1.2 Statement of the Problem.....	2
1.3 Research Questions.....	3
1.4 Objectives of the Study.....	4
1.4.1 General Objective the of Study.....	4
1.4.2 Specific Objectives	4
1.5 Significance of the Research.....	4
1.5.1 In Planning and Designing of Infrastructures	4
1.5.2 Flood Risk Assessment	4
1.5.3 Climate Change Adaption.....	5
1.5.4 Improved Emergency Responses	5
1.6 Scope of the Study	5
1.7 Research Limitations	6
CHAPTER 2: LITERATURE REVIEW	7
2.1 Previous Studies on Intensity Duration Frequency (IDF) Curves	7
2.2 Hydrological Data Preparation.....	9
2.2.1 Estimation of Missing Rainfall Data.....	9
2.3 Probability Distribution	10
2.3.1 Generalized Extreme Value (GEV)	10
2.3.2 Non-stationary Generalized Extreme Value Distribution	12
2.4 Parameter Estimation Technique	13
2.4.1 Least Square Method	14
2.4.2 Root Mean Squared Deviation (RMSD).....	15

2.4.3 Methods of Moments	15
2.4.4 Method of Maximum Likelihood.....	15
2.4.5 The L-moments	16
2.5 Goodness of Fit Test	17
2.5.1 Chi-Square Test	17
2.5.2 Kolmogorov-Simonov Fit.....	18
2.5.3 Anderson-Darling Test.....	18
2.6 Computation of Stationary and Non-Stationary Rainfall Extreme Intensities	18
CHAPTER 3: MATERIALS AND METHODS	19
3.1 Description of the Research Area	19
3.2 Software Used.....	20
3.2.1 ArcMap Software.....	20
3.2.2 Excel Sheet.....	21
3.2.3 R-Studio Software.....	21
3.3 Rainfall Data Collection	22
3.4 Estimation of Missing Data.....	22
3.4.1 Stationary-Year Method.....	22
3.4.2 Arithmetic Mean Method.....	23
3.4.3 Inverse distance weighted	23
3.5 Different Tests for Rainfall Data	23
3.5.1 Von-Neumann’s Independent Test	23
3.5.2 Evaluating Homogeneity with the Mann-Whitney’s Method.....	24
3.5.3 Test for Outliers	25
3.6 Disaggregation of Daily Rainfall into Shorter Durations	25
3.7 Trend Tests.....	26
3.7.1 Mann-Kendall Trend Test.....	26
3.8 Generalized Extreme Value Distribution (GEV).....	27
3.8.1 Stationary Generalized Extreme Value Models	28
3.9 Development of GEV Intensity Duration Frequency Curves	29
CHAPTER 4: RESULTS AND DESCUSSION.....	30
4.1 Preparation of Rainfall Data	30
4.1.1 Filling of the Missing Rainfall Data.....	30
4.1.2 Arithmetic Mean Method.....	31

4.2 Different Tests for Debre Markos Station Rainfall Data	31
4.2.1 Von-Neumann’s Independent Test	31
4.2.2 Testing for Homogeneity using Mann-Whitney’s Method	33
4.2.3 Test for Outliers	36
4.3 Disaggregation of Daily Rainfall Data into Shorter Durations	40
4.4 Calibration.....	41
4.5 Trend Test	44
4.5.1 Mann-Kendall Trend Test.....	44
4.5.2 R-Studio Trend Sample Test Results for Different Stations	47
4.6 Deriving Two, Three and Five Days Rainfall from Annual Maximum Daily Rainfall	48
4.7 Evaluation of Parameter Model Comparing Criteria	52
4.8 Evaluation of Time-Variat Parameter	53
4.9 Goodness of Fit Test	53
4.10 Development of GEV Stationary Models IDF Curves	55
4.11 Comparing ERA Regional and Stationary Model Rainfall Intensities	66
4.12 Validation for Rainfall	68
4.13 Validation for Rainfall Intensity	71
CHAPTER 5: CONCLUSION.....	76
CHAPTER 6: RECOMMENDATION	78
REFERENCES	79

LIST OF TABLES

Table 1: GEV Stationary Parameters Model.....	28
Table 2: Von-Neumann's Independent Test.....	32
Table 3: Mann-Whitney's Homogeneity Test.....	33
Table 4: Debre Markos Rainfall Station Rainfall Grubbs-Beck Outlier Test.....	37
Table 5: Debre Markos Station Rainfall Annual Maximum Disaggregated Rainfall.....	42
Table 6: Man-Kendall Trend Test.....	45
Table 7: Deriving Debre Markos Rainfall Station's Two, Three, and Five Days Rainfall from Annual Maximum Daily Rainfall.....	48
Table 8: Some Meteorological Rainfall Stations and Meteorological Regions.....	55
Table 9 :Debre Markos Station Rainfall GEV Distribution Fitted Stationary Intensity Levels (mm).....	56
Table 10 :Debre Markos Station Rainfall GEV Fitted Stationary Rainfall Intensity (mm/hr).....	56
Table 11: Bahir Dar Airport Station Rainfall GEV Fitted Stationary Return Levels (mm).....	59
Table 12: Bahir Dar Airport Station Rainfall GEV Fitted Stationary Rainfall Intensity (mm/hr).....	60
Table 13: Meshenti Station Rainfall GEV Distribution Fitted Stationary Return Levels (mm).....	62
Table 14 :Meshenti Station Rainfall GEV Distribution Fitted Stationary Rainfall Intensity (mm/hr).....	63
Table 15: Tisabay Station Rainfall GEV Fitted Stationary Return Levels (mm).....	64
Table 16: Tisabay Station Rainfall GEV Fitted Stationary Rainfall Intensity (mm/hr).....	65
Table 17: ERA Rainfall Intensity for Region A2 and A3 (mm/hr).....	66
Table 18: Debre Markos Station Rainfall Stationary Model Rainfall Intensity (mm/hr).....	67
Table 19: Comparison of Table 17 and Table 18 ERA and Debre Markos Station Rainfall Stationary Model Rainfall Intensities.....	67
Table 20: Comparison of Observed and Disaggregated Rainfall.....	69
Table 21: Exceedance Probability and Return Periods of Observed Rainfall.....	71
Table 22: Rainfall Intensity (mm/hr) Derived from Observed Rainfall Using Standard Equation.....	72
Table 23: GEV Distribution Fitted Disaggregated Intensity Levels (mm).....	73

LIST OF FIGURES

Figure 1: Map of Ethiopia Showing Study Area.....	20
Figure 2: Debre Markos Rainfall Station Rainfall Data Time Series	31
Figure 3: Debre Markos Rainfall Station Rainfall Data Outlier Plot.....	40
Figure 4: Moving Average Plots for Debre Markos Rainfall Station	51
Figure 5: Sample Rainfall Quantile Plot for 10 Minutes Duration	53
Figure 6: Sample Density Plot for Simulated and Fitted Rainfall Data.....	54
Figure 7: Debre Markos Station Rainfall Stationary Model Different Types of IDF Curves.....	58
Figure 8: ERA Rainfall Region A2 and A3 IDF Curves	59
Figure 9: Bahir Dar Airport Station Rainfall GEV Fitted Stationary Model IDF Curves	61
Figure 10: ERA Rainfall Region A2 IDF Curves	62
Figure 11: Meshenti Station Rainfall Stationary IDF Curves.....	64
Figure 12: Tisabay Station Rainfall GEV Distribution fitted Stationary IDF Curves	66
Figure 13: Validation for Rainfall Depth.....	70
Figure 14: IDF Curves from Observed Rainfall Data Using Standard Equation.....	72
Figure 15: IDF Curves from Disaggregated Rainfall Data	74
Figure 16: Observed and Disaggregated IDF Curves on the Same Normal Paper	75

LIST OF ABBREVIATIONS

IDF	Intensity Duration Curves
AMS	Annual maximum Series
MK	Mann-Kendall
EVT	Extreme Value Theory
GEV	General Extreme Value
GEV1	General Extreme Value Type-I
GEV2	General Extreme Value Type-II
GEV3	General Extreme Value Type-III
CDF	Cumulative Distribution Function
PDF	Probability Density Function
NAMA	National Meteorological Agency
SM	Stationary Model
NS	Non Stationary
AIC	Akaike's Information Criteria
AICC	Corrected Akaike's Information Criteria
BIC	Bayesian Information Criteria
N	North Direction
E	East Direction
WMO	World Meteorological Organization
EMA	Ethiopian Meteorological Agency
ERA	Ethiopian Roads Authority

CHAPTER 1: INTRODUCTION

1.1 Background

In the hydrological cycle, rainfall is one of the most important elements. The estimation of rainfall occurrences is therefore necessary for the planning and design of all hydrologic projects, including storm and drainage systems, geotechnical and structural projects, and water resources systems (Chitrakar et al., 2023). In order to guarantee safe design and financial sustainability for hydrologic and engineering projects over a specified time period, intensity duration frequency curve analysis is used as a tool to quantify rainfall (Chow, 1988).

Around the world, a large number of professionals in the fields of engineering, hydrology, and environmental studies have created several kinds of intensity duration frequency correlations (Chitrakar et al., 2023). Probability distribution was used to develop the mathematical basis for IDF curves using rainfall data from both recording and non-recording sites.

One of the most widely used instruments for planning and creating different engineering urban infrastructure systems, such as flood protection structures and urban drainage infrastructures, is the intensity duration frequency curve. The intensity duration frequency curves in the GEV stationary model are produced using stationary frequency analysis of historical annual maximum rainfall for a specific duration, taking into account the idea that the frequency of extreme precipitation events stays constant throughout time (Silva et al., 2021).

Comprehending the correlation between rainfall intensity, duration, and frequency curves (IDF) is therefore a commonly utilized tool for a number of engineering projects in order to prevent and mitigate flooding. Intensity duration frequency curves require automated rainfall data with sub-hourly and hourly intervals in addition to a history record of maximum rainfall data with very fine resolution. The primary goal of this study was to apply the stationary approach to generate intensity duration frequency curves for the town of Merawi, Ethiopia, after determining that there was no non-stationary trend.

1.2 Statement of the Problem

The town's growth transformed the naturally occurring land surfaces into impermeable ones including roads, parking lots, walkways, and various pavements. This drastically reduced the rate of infiltration and increased the volume of surface runoff from precipitation, which causes flooding, erosion, and habitat degradation (Simeneh Melesse, 2016).

Ethiopia is geographically separated into several distinct rainfall areas; nonetheless, it would be ideal if each town or locality had its own version. Because of this, the existing design guidelines for rainfall intensity duration frequency curves created by ERA regional intensity duration frequency curves for Ethiopia don't take into account the variations in climate experienced by individual towns, as well as the impact of urbanization and altitude (Tariku Tegenu, 2021). Due to Merawi Town's precipitation patterns being either greatly overestimated or underestimated, the chance of floods and the resulting damage to infrastructure are increased, which raises the cost of infrastructure construction.

To create a more effective and efficient water management system, better rainfall modeling that considers the town's location changes and variations in rainfall patterns is important. The construction of a dependable storm water management system is difficult in Merawi Town due to the high degree of rainfall pattern fluctuation. Consequently, it became imperative to choose a strategy that uses probabilistic models to better account for the variability in rainfall duration and to build a system that can estimate extreme events for every town.

These days, engineers build infrastructure at Merawi Town using the ERA regional intensity duration frequency curves developed from various towns, including Addis Ababa, Gonder, Debrezeit, Fitcha, and others. However, because rainfall intensities vary with location and altitude, this can lead to under- or overestimation and neglect to take into account various rainfall characteristics. Because of the underestimation of the rainfall design estimated from the regional IDF, this leads to road flooding. Thus, if there is no pattern in the rainfall data, stationary methods should be used to construct intensity duration frequency curves for each municipality in order to control floods over roadways, parking walks, and other payment structures.

These are the justifications for studying the daily, hourly, and sub-hourly IDF curves for Merawi Town using the stationary method of IDF curve development method. By building various hydraulic and hydrologic structures, the town and surrounding area can be controlled from flooding. Using various durations and return periods of the design flood, intensity for Merawi Town can be effectively quantified by creating intensity duration frequency curves using daily, hourly, and sub-hourly rainfall data. When designing the drainage and other water infrastructure in Merawi Town and the surrounding areas, short duration IDF curves are preferable to ERA regional IDF and daily IDF.

1.3 Research Questions

- ❖ What methods are used to evaluate the quality of daily, hourly, and sub-hourly rainfall data for Merawi Town, Ethiopia?
- ❖ How the General Extreme Value (GEV) distribution fitted rainfall intensities change in stationary models at different durations and return periods?
- ❖ How the IDF of the GEV distribution fitted rainfall intensities for stationary models at Merawi Town, Ethiopia will be developed?
- ❖ How comparable are the IDF curves developed by GEV fitted stationary model and IDF curves developed by ERA regional curves method?

1.4 Objectives of the Study

1.4.1 General Objective the of Study

The main objective of this thesis work is to develop rainfall intensity duration frequency (IDF) curves for Merawi Town, Ethiopia by using stationary method.

1.4.2 Specific Objectives

- ❖ To evaluate the quality of Merawi Town's daily, hourly, and sub-hourly rainfall data using various techniques such a Mann-Kendall, Mann-Whitney, Von-Neumann methods
- ❖ To develop General Extreme value distributions fitted rainfall intensities using stationary models for Merawi Town, Ethiopia
- ❖ To develop rainfall intensity-duration-frequency (IDF) curves for the developed stationary model rainfall intensity
- ❖ To evaluate the differences between stationary and ERA regional method computed IDF rainfall intensities

1.5 Significance of the Research

The following are some of the reasons why Merawi Town, Ethiopia, needs to develop intensity, length, and frequency:

1.5.1 In Planning and Designing of Infrastructures

Storm water management infrastructures, such as retention ponds, culverts, and drainage systems, can be designed to efficiently convey, control, and treat runoff from rainfall events. This can be done with the help of rainfall modeling, which can be used for both shorter and longer periods of time.

1.5.2 Flood Risk Assessment

The town's possible flood risk can be evaluated with the use of IDF curves, which can help prioritize mitigation efforts and reducing the effects of subsequent flooding incidents.

1.5.3 Climate Change Adaption

The creation of IDF curves can also help with the development of adaptive strategies to reduce the effects of extreme events by offering pertinent information on changes in rainfall patterns and intensities brought on by climate change.

1.5.4 Improved Emergency Responses

By carefully creating IDF curves, emergency response teams may make informed decisions about how serious and long rainfall events will last, which will help them set priorities and manage resources. The development IDF curves of the short duration design rainfall for Merawi town in particular can help with better infrastructure planning and design, more effective and efficient management of water resources, raising awareness of the effects of climate change, and, ultimately, a reduction in the likelihood of flooding.

1.6 Scope of the Study

The development of precipitation events, such as the intensity of rainfall at Merawi, Ethiopia, was the main focus of this study.

The scope of this thesis investigation is restricted to the development of IDF curves that simulate rainfall events in order to better understand the effects of maximum rainfall events on the town's potential for flooding. In addition, the task of creating rainfall intensity duration frequency curves for stationary rainfall data analysis in order to figure out the intensity of the rainfall for the selected stations at different return periods is limited. Equation $R_t = R_{24} \left(\frac{t}{24}\right)^{\frac{1}{3}}$ was used to disaggregate the respective rainfall of each station to smaller values. It did not address other forms of estimating hazard events, such landslides or structural dimensions. The primary goals of the research were to create General Extreme value distributions of rainfall intensities for stationary models for the Merawi town, Ethiopia, focused areas, which could be used to predict rainfall events and manage the town's flood risk. Secondly, the research created Rainfall intensity duration frequency curves for stationary models.

1.7 Research Limitations

One of the research's limitations was the lack of rainfall data, such as observed daily, hourly, and sub-hourly rainfall data from very close stations, which was necessary for validation and calibration. Another was the lack of a long enough record of metrological rainfall data for neighboring stations. It was difficult to specifically get the necessary amount of rainfall in a year, software, and data for calibration and validation.

Although it was a good idea to develop IDF curves from nearby stations within a 25–30 km radius from the study area with large rainfall recodes, it became necessary to do so because there were no long historical rainfall records. In addition, some recent literature advised using climate data up to 150 km, so four relatively nearby stations in the same rainfall ERA region with better rainfall records were used. It was a difficult effort to handle the observed hourly, sub-hourly, and daily rainfall data for calibration and validation; it was also difficult to access the necessary time series. In addition, the research was conducted during an undesirable time because of the disparities in security across the nation, which hindered the data collection process.

CHAPTER 2: LITERATURE REVIEW

2.1 Previous Studies on Intensity Duration Frequency (IDF) Curves

Intensity Duration Frequency (IDF) curves graphically depict the link between rainfall intensity duration frequencies and are utilized in the design and evaluation of storm water management, flood control, and water delivery systems. The ability to evaluate the distribution of rainfall intensity over a range of time intervals is a crucial tool for hydrologists, water resources engineers, and planners. A mathematical function is fitted to the rainfall data gathered over a predetermined amount of time in order to create an IDF curve (Rodríguez-Solà et al., 2017).

For civilization to develop sustainably, the design of hydraulic structures such as drainage systems, culverts, bridges, and dams is crucial. Hydrologic modeling of these structures uses design rainfall as one of its main input parameters. Determining the frequency, intensity, and duration of rainfall is necessary for an accurate estimate of design rainfall.

Short duration rainfall events, usually lasting less than two hours, account for a sizable portion of yearly rainfalls in many regions of the world and are a crucial factor in determining the runoff response of a catchment. Hydraulic structure design and management are greatly influenced by the evolution of rainfall events.

Intensity-duration-frequency (IDF) curves graphically illustrate the relationship between rainfall intensity, duration, and return time. In civil engineering and hydrology, they are used in the design of storm water drainage systems, flood control structures, and other hydraulic infrastructure (Tanchev, 2014).

When engineers and hydrologists started researching the long-term rainfall records of various regions in the early 1900s that is when IDF curves were first developed. They discovered that there was a statistical distribution in the intensity of rainfall events, with the most intense rainfall happening less frequently.

As a result, the idea of the return period the mean interval between rainfall events of a specific intensity was developed. The US Army Corps of Engineers created the Gamble method, a statistical technique for creating IDF curves, in the 1940s. This technique is still in use today. Plotting the annual maximum rainfall intensity for various durations on a logarithmic scale is the

Gamble method's method. Following the fitting of the plot's points to a statistical distribution, the return periods for each intensity were calculated (Pawar et al., 2023).

Data from a select few rainfall locations in the eastern United States served as the foundation for these curves. A more thorough collection of IDF curves covering the whole country was created in the 1940s by the U.S. Weather Bureau. The data used to create these curves came from more than 1,000 rainfall stations. IDF curves were created in the 1950s and 1960s for numerous additional nations. These curves were created using information from each nation's rainfall stations (WMO, 1978).

It is possible that IDF curves in Ethiopia were created throughout time to account for the unique hydrological and climatic circumstances of the nation. Ethiopia's geography varies, resulting in various rainfall patterns in different areas. Consequently, in order to forecast rainfall intensities, durations, and frequencies with any degree of accuracy across the nation, unique IDF curves would be required.

The Ethiopian Meteorological Agency (EMA) created the initial IDF curves for Ethiopia in the 1970s. The data from a select few Ethiopian rainfall stations served as the basis for these curves. A more complete collection of IDF curves for Ethiopia was created by the EMA in the 1990s. These curves were created using information from more than 100 Ethiopian rainfall stations (EMA, 1990). Yohannes Gerezihier Gebremedhin created IDF curves for the Somali region in 2017, while Simeneh Gebeyehu Melese created IDF curves for Bahir Dar City in 2016 using a straightforward scaling method. Along with the aforementioned researchers, Moges Tarku Tegenu and Eyoel Yigletu Aybehon also developed IDF curves for Wolkite Town and the North Shoa Amhara region in 2021 and 2022, respectively.

The ERA Drainage Manual, published in 2002, established intensity duration frequency curves for commonly designed frequencies by employing statistical analysis on six regimes or regional areas based on rainfall stations (Simeneh Melesse, 2016). This thesis work employed the GEV stationary approach principles to build the IDF for Merawi tow, prioritizing the consideration of possible trend presence. Using R-studio software, the distribution parameters for determining the rainfall value at the necessary duration and return period were computed using the general extreme value estimator method.

2.2 Hydrological Data Preparation

2.2.1 Estimation of Missing Rainfall Data

To create IDF curves from rainfall data, a sufficiently lengthy rainfall record is required. Missing of precipitation Data can appear for a variety of reasons, including when a rain gauge breaks and is unavailable for a few days or weeks, during construction, during plant planting, when the rain gauge is relocated, and for other reasons. When required, the following techniques are used to estimate the missing record (Raghunath, 2006).

2.2.1.1 Stationary-Year Method

The records of two or more stations are combined into a single, longer record, with each station's data remaining independent and the stations' locations sharing the same climate. This method uses a ratio of average or graphical comparison to find the missing records in the station for a specific year. The outcome can be verified by comparing it to another nearby station (Raghunath, 2006).

$$\frac{A_y}{A_a} = \frac{B_y}{B_a} \dots\dots\dots (1)$$

The total rainfall at station A in a given year is denoted by A_y , the annual average at station A is by A_a , the total rainfall at station B is by B_y , and the annual average at station B is by B_a .

2.2.1.2 Arithmetic mean method

If the normal annual precipitation of the neighboring stations is within 10% of the normal annual precipitation of the station without a record, the missing record is calculated using the arithmetic mean approach (K.Subramanya, 2005).

The arithmetic mean method is recommended for estimating missing data in locations where the annual rainfall variance between stations is less than 10% (Dingman, n.d.).

$$P_x = \frac{1}{M} (P_1 + P_2 + P_3 + \dots + P_n) \dots (2)$$

Whereas M is the number of precipitations, and P_i is the annual precipitation at the nearby station.

2.2.1.3 Normal Ratio Method

If the annual normal precipitation at nearby stations is greater than 10% of the annual normal precipitation at the station where the record is missing, then normal ratio method can be used (Chaw, 1988).

$$Px = \frac{Nx}{M} \left(\frac{P1}{N1} + \frac{P2}{N2} + \dots + \frac{Pm}{Nm} \right) \dots (3)$$

Where M is the number of nearby stations Pm is the normal annual precipitation Nm is the normal annual precipitation at different sites.

2.2.1.4 Inverse Distance Weighted

It is a better approach because monthly climate data specifically fluctuates with distance, and the distance between stations will be considered (Sattari et al., 2017).

$$Px = \frac{\sum_{i=1}^n \frac{Pi}{Di}}{\sum_{i=1}^n \frac{1}{Di}} \dots \dots \dots (4)$$

Where Pi is the amount of precipitation at nearby stations and Di is the distance between stations.

The frequency Different probability distribution techniques are used in the analysis of hydrological data to relate the frequency of extreme events to their magnitude. It is considered that a hydrological event will follow a specific distribution type, such as the general extreme value, log Pearson, log normal, or gamble distribution (Htun & Thein, 2019).

2.3 Probability Distribution

2.3.1 Generalized Extreme Value (GEV)

The generalized extreme value is composed of probability distributions that fuse three asymptotic extreme value distributions into one, based on the limit theorem for blocking maximum or minimum. Gumbel (GEV1), Frechet (EV2), and Weibull (EV3) make up this group (Shamkhi et al., 2022).

2.3.1.2 Gumbel Extreme Value Distribution

The Gumbel distribution is used to generate a range of extreme behaviors using the three distribution parameters location, scale, and shape. The location parameter describes the

distribution change in each direction along the horizontal axis. The scale parameter describes the degree of dispersion of the distribution and the position of its center. The shape parameter, which is dictates the distribution's skewness, and affects the properties of the tail. It is shown that the shape parameter is equal to zero and that the light tail is a Gambled distribution. The Frechet (EV2) distribution has a heavy tail if the shape parameter value is more than zero, whereas the Weibull distribution has a short tail if the shape parameter value is less than zero(Shamkhi et al., 2022).

In addition to analyzing monthly and yearly maximum values of daily rail fall and river discharge measurements, the Gumbel distribution is also used to characterize droughts. For the extreme maxima and minima of hydrological variables, the Gumbel distribution is employed(Htun & Thein, 2019). The Gamble distribution for the rainfall (PT) that corresponds to a specific return period (T) is as follows:

$$P_T = \sigma + KS \dots (5)$$

In this formula, σ represents the average yearly daily maximum rainfall, S the standard deviation of the daily maximum rainfall, T the return period, and K the frequency factor.

$$K = \frac{-\sqrt{6}}{\pi} (0.5772 + \ln(\ln(\frac{T}{T-1}))) \dots (6)$$

2.3.1.3 Log-Pearson Type III

The Log-Pearson III distribution is a frequently employed technique for frequency analysis, as it is the foundational approach advocated by the US Water Resources Council.

Furthermore, according to the Water Resource Council, statistical characteristics like mean, standard deviation, and coefficient of skewness of the logarithm of rainfall data should be used to fit this distribution to the sample. Phien and Jivajirah (1984) applied the log Pearson type III distribution to the yearly maximum rainfall and annual stream flow in the previous year(Htun & Thein, 2019). Equations for calculating the Log-Pearson Type III distribution are as follows:

$$PT = Pave + K_T S_i$$

$$P_{ave} = \frac{1}{n} \sum_{i=1}^n P_k$$

$$P_k = \log (P_i)$$

$$S_i = \left[\frac{1}{n} \sum_{i=1}^n (p_k - p_{av})^2 \right]^{\frac{1}{2}} \dots \dots (7)$$

Where, P_T =logarithmic extreme value of Rainfall

P_{ave} =average of maximum precipitation corresponding to specific duration

S =standard deviation of P_k data

K_T =Pearson frequency factor it depends on T and skewness coefficient C_s

The skewness coefficient is necessary to get frequency factor and it is computed by the equation:

$$C_s = n \sum_{i=0}^n \frac{(P_k - P_{ave})^3}{(n-1)(n-2)(S)^3} \dots \dots \dots (8)$$

2.3.1.3 Normal distribution

The normal distribution is used for frequency analysis, data simulation, and fitting an empirical distribution to hydrological data. Regularly, the normal distribution is used to draw statistical conclusions (Shamkhi et al., 2022). The probability density function for x variable with a normal distribution is provided by:

$$f(x) = \frac{1}{\delta\sqrt{2\pi}} e^{\frac{-1}{2\sigma^2}(x-\mu)^2} \dots \dots \dots (9)$$

Where the distributional parameters are denoted by μ and δ . In the ranges $(-\infty, \infty)$, the variable x can have any value. A standard normal variable is one whose standard deviation is equal to one and its mean is equal to zero (Simeneh Melesse, 2016).

2.3.2 Non-stationary Generalized Extreme Value Distribution

Extreme Value Theory (EVT) offers a strong foundation for studying climate extremes and their return levels. The distribution of the maxima or minima converges to one of three limiting distributions, such as the Gumbel, Frechet, or Weibull distributions, under a wide range of

conditions. These distributions combined make up the generalized extreme value (GEV) distribution family.

With the flexibility of the GEV distribution, the three distribution parameters (μ , δ , ξ) enable the development of different modeling behaviors of extremes. The scale parameter (δ) controls the magnitude of the deviation around the location parameter, the shape parameter (ξ) determines the behavior of the GEV distribution's tail, and the location parameter (μ) indicates the distribution's center.

Gumbel's distribution is shown in the limiting case of $\xi \rightarrow 0$, the Frechet distribution is shown in $\xi > 0$, and the Weibull distribution is shown in $\xi < 0$ (Linyin Cheng, 2014).

In this study, the term "stationary" refers to extreme qualities that are time invariant, while the phrase "non-stationary process" refers to underlying distribution function parameters that are time dependent and distribution properties that change over time.

The annual maxima are modeled using the Generalized Extreme Value (GEV), and the GEV cumulative distribution is given by the following equation (Lalani Jayaweera, 2023):

$$F(X) = \exp\left\{-\left[1 + \frac{\xi(X-\mu)}{\delta}\right]^{-\frac{1}{\xi}}\right\}, \text{ for } \delta > 0, 1 + \frac{\xi(X-\mu)}{\delta} > 0, \xi \neq 0 \dots \dots \dots (10)$$

$$F(x) = \exp\left\{-\exp\left[-\left(\frac{x-\mu}{\delta}\right)\right]\right\}, \delta > 0, \xi = 0$$

Where X is the highest annual rainfall and μ , δ , and ξ stand for the shape, scale, and location parameters, respectively. Such that $-\infty < \mu < \infty$, $\delta > 0$ and $-\infty < \xi < \infty$,

The following formula yields the quantile (QP) estimates of the yearly maximum distribution:

$$QP = \mu - \frac{\delta [1 - \{-\log(1-p)\}^{-\xi}]}{\xi} \text{ For } \xi \neq 0$$

$$QP = \mu - \delta \log \{-\log(1-p)\} \text{ for } \xi = 0 \dots \dots \dots (11)$$

ΔQ_p represents the extreme rainfall rising at the given rate, and is computed by

$$\Delta Q_p = \Delta \mu - \frac{\Delta \delta [1 - \{-\log(1-p)\}^{-\xi}]}{\xi} \text{ for } \xi \neq 0 \dots \dots \dots (11)$$

$$\Delta QP = \Delta \mu - \Delta \delta \log \{-\log(1-p)\} \text{ for } \xi = 0$$

2.4 Parameter Estimation Technique

The process of determining a model's parameter values that best suit the observable data is known as parameter estimation. This is a basic statistical problem, and there are numerous

approaches to parameter estimate, each with pros and cons of their own. Several of the most popular techniques are as follows.

2.4.1 Least Square Method

The most popular method for estimating parameters is this one. By doing so, the total of the squared errors between the model's predictions and the observed data is reduced.

It is employed to investigate the connection between two variables. The least squares method is a more precise means of determining the line of best fit. The parameters of x and y for the creation of empirical equations correlated with rainfall intensity and duration are determined using the least squares approach.

To get the empirical equation with the best match intensity duration frequency, one uses the correlation coefficient (R). The best fit equation for the provided return period is one that yields a R value close to 1, and the best approximation of the given data set is a straight line, which is known as the line of best fit(Htun & Thein, 2019).

$$y = ax + b \dots\dots (15)$$

$$a = \frac{rsx}{sy}$$

$$b = \bar{y} - a\bar{x}$$

Where, r= coefficient of correlation

y= least squares regression line

a= the regression line's slope

b= the y-axis and the regression line's intercept point

\bar{x} = average of the value x

\bar{y} = average of the value of y

S_x = the x-standard deviation

S_y = the y value's standard deviation

2.4.2 Root Mean Squared Deviation (RMSD)

The square root of the sum of the squared deviations between the actual and predicted amounts of rainfall, divided by the total number of observations, yields the root mean square deviation (RMSD) (Petitjean, 1999). The lower the RMSD score, the more accurate the prediction is.

$$RMSE = \frac{\sqrt{(\sum(\text{observed} - \text{predicted})^2)}}{n} \dots (16)$$

Where: the number of observations (n), the actual rainfall amount (observed), and the expected rainfall amount (predicted)

2.4.3 Methods of Moments

The moments of the probability density function about the origin are approximated as the parameters of a probability distribution when they match the corresponding moments of the sample data. If the data value are each assigned a hypothetical mass equal to their relative frequency of occurrence ($\frac{1}{n}$) it is imagined that this system of mass is rotated about the origin $x=0$, then the first moment of each observation x_i about the origin is equal to the product of its moment arm x_i and its mass $\frac{1}{n}$, and the sum of these moments overall the data is given below

(Chaw, 1988).

$$\sum_{i=1}^n \frac{x_i}{n} = \frac{1}{n} \sum_{i=1}^n x_i = \bar{X} \dots\dots\dots (17)$$

The initial moment regarding the origin = $\sum_{n=1}^{\infty} \left(\frac{x_i}{n}\right) = \bar{X}$

The moments method Choose the probability density function's parameter values such that the sample data's moments match the functions. The probability density function's associated centroid is equal to:

$$\mu = \int_{-\infty}^{\infty} x f(x) dx \dots\dots (18)$$

2.4.4 Method of Maximum Likelihood

The optimal value should be applied to the parameter in the probability distribution function that maximizes the joint probability of the observed sample's occurrence. If the sample space is partitioned into intervals of length dx and a sample of independent and identically distributed observations x_1, x_2, \dots, x_n is chosen, then the probability density function $X=x_i$ is equal to $f(x)$.

$F(x) dx$ is the probability that the random variable will occur in the interval containing x_i . Given the independence of the data, the product $f_1(x) dx f_2(x) dx \dots f_n(x) dx = \prod_{i=1}^n f(x_i) dx^n$, determines the joint probability of occurrence of the observations. Maximizing the likelihood function is equivalent to maximizing the joint probability of the observed sample because the interval size dx is fixed (Chaw, 1988).

$$L = \prod_{i=1}^n f(x_i) \dots \dots \dots (19)$$

Because many probability functions are exponential, there are situations when working with the log likelihood function is more convenient.

$$\ln L = \sum_{i=1}^n \ln[f(x_i)] \dots \dots \dots (20)$$

2.4.5 The L-moments

Probabilities weighted moments are modified to create L-moments, which are then used to estimate easily interpreted parameters. An effective replacement for the moments of distributions is the L-moment, which is a linear combination of the order of statistics of the annual maximum rainfall quantity (Schardong et al., 2020). The probability weighted moments can be estimated using the following equation:

$$w_0 = n^{-1} \sum_{j=1}^n x_j \dots \dots \dots (21)$$

$$w_1 = n^{-1} \sum_{n=2}^n \left(\frac{j-1}{n-1}\right) x_j \dots \dots (22)$$

$$w_2 = n^{-1} \sum_{n=2}^n \frac{(j-1)(j-2)x_j}{(n-1)(n-2)} \dots \dots (23)$$

The ordered sample of the annual maximum series is denoted by x_j , while the initial probability weighted moments are represented by w_i .

The sample moments can then be calculated using the following formulas.

$$m_1 = w_0 \dots \dots \dots (24)$$

$$m_2 = 2w_1 - w_0 \dots \dots (25)$$

$$m_3 = 6w_2 - 6w_1 + w_0 \dots \dots (26)$$

The following formula is used to determine the shape (ξ), scale (δ), and position (μ) of the GEV parameters:

$$\xi = 2.9554rc^2 + 7.8590c \dots (27)$$

$$c = \frac{2}{3 + \frac{m_3}{m_2}} - \frac{m_2 n}{m_3 n} \dots \dots \dots (28)$$

$$\delta = \frac{m_2 \xi}{(1 - 2^{-\xi}) \cdot \Gamma(1 + \xi)} \dots \dots (29)$$

$$\mu = m_1 - \delta \frac{((1 - \Gamma(1 + \xi)))}{\xi} \dots \dots (30)$$

The parameters of the GEV distribution are location (μ), scale (δ), and shape (ξ), and the first three moments are represented by m_1 , m_2 , and m_3 in $\Gamma(\cdot)$ the gamma function.

2.5 Goodness of Fit Test

The degree to which sample rainfall data aligns with the theoretical probability distribution is determined by the goodness of fit test. The null hypothesis is tested using the goodness of fit (Mohita Anand & Jai Bhagwan, 2010).

HO: The data on the maximum daily rainfall correspond to a particular distribution.

HA: The data on the maximum daily rainfall does not correspond to a particular distribution.

2.5.1 Chi-Square Test

A chi-squared test is a statistical hypothesis test that is used to evaluate how well the expected and observed frequencies in a contingency table correspond. The purpose of the test is to ascertain whether the observed and anticipated frequencies differ statistically significantly.

Statistical significance is often defined as a p-value of less than 0.05. This indicates that, should the null hypothesis hold true, there is a chance of less than 5% to acquire the observed chi-squared statistic. It is crucial to remember that small sample sizes may cause the test to become sensitive. A small sample size may prevent the chi-squared test from identifying a true relationship between the two variables (Simeneh Melesse, 2016).

$$\chi^2 = \sum_{i=1}^k \frac{(O_i - E_i)^2}{E_i} \dots \dots \dots (31)$$

The variables E_i and O_i represent the expected and observed frequencies, respectively, and i , the number of observations (1, 2... k). E_i is calculated as $E_i = F(x_2) - F(x_1)$

F = CDF of the probability distribution under examination

The formula is used to calculate the observed number of observations (k) in the interval i.

$$K = 1 + \log 2n \dots (32)$$

2.5.2 Kolmogorov-Simonov Fit

Simonov-Kolmogorov The fit statistic measures how much the theoretical and empirical cumulative distribution functions differ vertically (Mohita Anand & Jai Bhagwan, 2010). For simplicity it is symbolized by letter D.

$$D = \max \left[F(xi) - \frac{i-1}{n}, \frac{i}{n} - F(xi) \right], 1 \leq i \leq n \dots (33)$$

For each $i = 1, 2, \dots, n$, and $x_i =$ random sample

$$CDF = F_n(x) = \frac{1}{n} [\text{number of observations} \leq x] \dots (34)$$

2.5.3 Anderson-Darling Test

The test compares the best fit of an observed cumulative distribution function to a predicted cumulative distribution function, giving tails more weight than the Kolmogorov-Simonov fit (Mohita Anand & Jai Bhagwan, 2010).

The following equation represents the statistics A_2 of the Anderson-Darling Test.

$$A_2 = -n - \frac{1}{n} \sum_{i=1}^n (2i - 1) * [\ln F(x_i) + \ln(1 - F(X_{n-i+1}))] \dots (35)$$

2.6 Computation of Stationary and Non-Stationary Rainfall Extreme Intensities

If the cumulative distribution function is inverted, one can obtain the formula for calculating the extreme intensity of stationary rainfall (Haruna et al., 2023).

$$X_T = \mu - \frac{\delta}{\xi} \left[1 - \left\{ -\ln \left(1 - \frac{1}{T} \right) \right\}^{-\xi} \right] \text{ for } \xi \neq 0 \dots (12)$$

However, the following formula is employed to determine the non-stationary rainfall intensities:

$$X_T = \bar{\mu} + \frac{\delta}{\xi} \left(\left(-\frac{1}{\ln p} \right)^\xi - 1 \right) \text{ for } \xi \neq 0 \dots (13)$$

$$\bar{\mu} = Qk(\mu_1, \mu_2, \mu_3 \dots \mu_n) \quad \mu(t) = \mu_1 t + \mu_0 \dots (14)$$

Where T is the return duration and X_T is the rainfall intensity exceedance value.

CHAPTER 3: MATERIALS AND METHODS

3.1 Description of the Research Area

Merawi is a town in northern Ethiopia's Amhara region, serving as the capital of Mecha Woreda. Near the north of the town lies Lake Tana, Ethiopia's largest lake, this is renowned for both its scenic beauty and its historical sites.

The Town's streets are lined with vintage houses and tiny shops, giving it a relaxed, rural vibe. The capital of Ethiopia, Addis Ababa, is 530 kilometers away from Merawi, which is 35 kilometers south of Bahir Dar. At a height of 1901 meters above mean sea level, the location is exactly 7 kilometers from the Koga dam. Its GPS coordinates are located between latitudes $11^{\circ}24'30''\text{N}$ and $11^{\circ}25'30''\text{N}$ and longitudes $37^{\circ}9'0''$ and $37^{\circ}10'0''\text{E}$, respectively.

The average yearly temperature and annual rainfall in the town are 20 to 30 °C and 1200 to 1800 mm, respectively. Rainfall is highest during the summer months, which start almost in mid-June and end in September (Lewoyehu, 2021).

The Study area is located in the typical climatic zones of Weynadega and Dega. The Weyna Dega climatic area enjoys moderate to warm, semi-humid weather with averages exceeding 20°, whereas the Dega area has a cool, humid climate with mean annual temperatures ranging from 10° to 20°.

Merawi Town is the starting point of Koga watershed, which is located in the Lake Tana sub-basin in the eastern portion of the Blue Nile River. It also denotes the settlement of north Mecha Woreda. From the mountainous area, the Koga watershed drains to the Gilgel Abay River, which eventually empties into Lake Tana.

High runoff and related silt flow from the top part of this watershed negatively affect the people who reside downstream of this river and the Koga irrigation reservoirs. The lush land surrounding the town and agriculture provide a living for the bulk of the population. In the past, people cultivated crops like teff, coffee, and maize (WaterAid, 2018). Consequently, identifying floods as a significant and persistent issue that has impacted the Town is now required. Flooding damage has endangered the town's economy and social stability in addition to causing property and infrastructure losses.

Developing successful ways to mitigate these hazards requires a thorough understanding of the underlying causes of floods in a town.

As a result, Merawi has a highland subtropical climate. This suggests that, with colder circumstances at higher elevations, the year-round temperature is somewhat mild. The Town normally has a very rainy season from June to September; the remaining months of the year are predicted to be dry. Due to the higher elevation, the temperature can fluctuate but generally stays moderate.

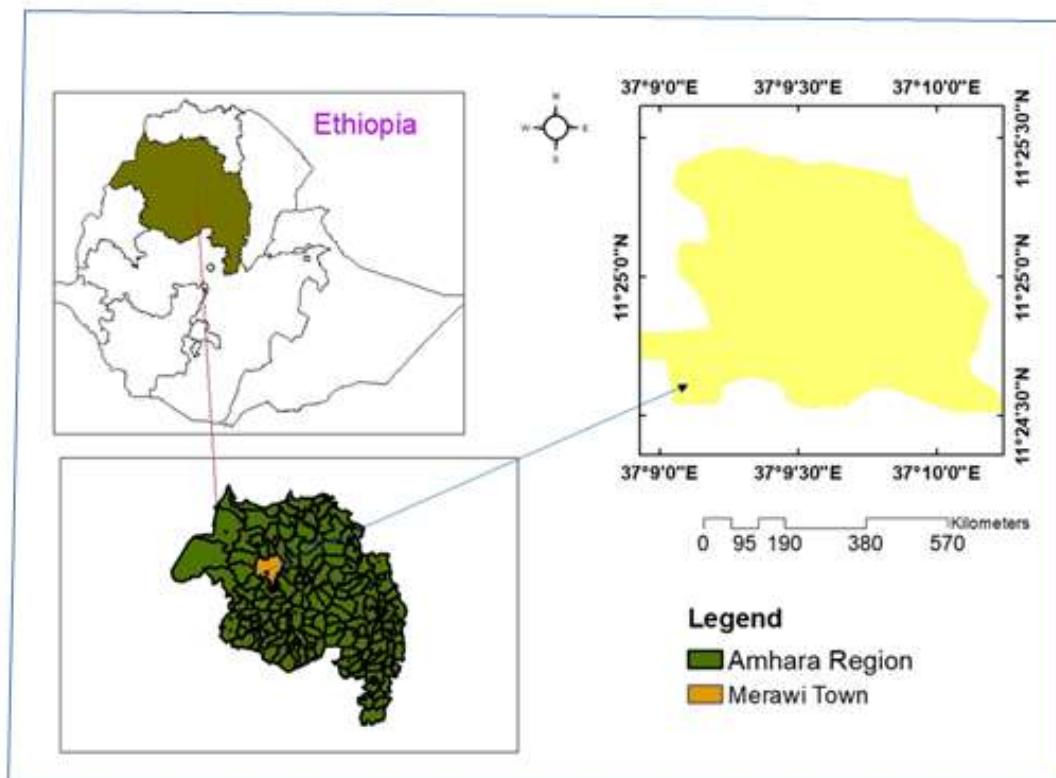


Figure 1: Map of Ethiopia Showing Study Area

3.2 Software Used

3.2.1 ArcMap Software

It contains specific tools for managing, organizing, deciphering, and presenting unique or geographical data. It facilitates the creation, storing, processing, analysis, and presentation of geographic and special data pertaining to certain spots on the surface of the earth.

Users of ArcMap software can build maps and visual representations of geographic data. To successfully convey special information, it offers a variety of symbolic possibilities, such as labels, colors, and symbols. Thematic maps, 3D representations, and interactive(Wallace, 2005).

3.2.2 Excel Sheet

Excel allows users to arrange and work with data in rows and columns through a grid-like interface. It accepts several types of data, such as dates, numbers, messages, and formulas. Excel has numerous sets of built-in formulas and functions for a range of mathematical applications.

Users are able to perform fundamental arithmetic operations including addition, subtraction, multiplication, and division in addition to too complex statistics and mathematical procedures. Among the data analysis tools Excel offers are data sorting, filtering, and pivot table creation. Additionally, Excel users can impose constraints and limitations on data submission via data validation rules, which incorporate criteria like data type, range, or practical formula(Wallace, 2005).

3.2.3 R-Studio Software

Specifically designed for the R programming language, R-Studio is an integrated environment.R is a potent open-source programming language and software environment for graphics and statistical computing.

R-Studio offers several functions based on the type of assignment. R code can be written, edited, and run in an interactive environment with a code editor. To manage objects, data, and packages in a R session, R-Studio offers a workspace pan. Users may view and edit data frames, variables, and other objects with it. It is easy to remember and re-use the code because the history pan maintains track of previously run R commands. R-Studio comes with a built-in package management facility. Users can install, update, and remove packages from CRAN, a vast R archive network, and other sources using its package management feature.

Additionally, R-Studio offers an interface for loading packages into the R session and managing package dependencies. Plots and visualizations can be created and viewed on a special pan in R-Studio. It is compatible with multiple R graphical packages, such as lattice, ggplot2, and simple graphics. Plots can be interacted with, settings changed, and exported in various formats by users(Lock, 2014).

3.3 Rainfall Data Collection

For this study, rainfall and geographic data were collected. The rainfall data's daily recorded values were then converted into other formats, like the annual maximum daily and total annual rainfall values, based on particular requirements and procedures.

When choosing the rainfall station, several variables were taken into account, such as its ability to automatically record rainfall, the duration of its record for a given year, and its environmental resemblance to the research area.

The Ethiopian Meteorological Agency (EMA) provided daily rainfall statistics according to the station's previously stated standards. After sorting the rainfall recordings, the corresponding durations and millimeter amounts of rainfall were recorded. The annual maximum daily rainfall depth for each year was extracted from the sorted data.

3.4 Estimation of Missing Data

For the examination of rainfall data frequency, a sufficiently lengthy record is required. A rain gauge may stop working for a day or a month due to malfunctions, building, planting, transferring the gauge to a different location, and other circumstances. This results in missing rainfall data (Raghunath, 2006). The missing record is estimated using the following methods.

3.4.1 Stationary-Year Method

The records of two or more stations are combined into a single, longer record, with each station's data remaining independent and the stations' locations sharing the same climate. This method uses a ratio of average or graphical comparison to find the missing records in the station for a specific year. The outcome can be verified by comparing it to another nearby station (Raghunath, 2006).

$$\frac{A_y}{A_a} = \frac{B_y}{B_a}, \dots \dots (1)$$

Where A_y is the total amount of rainfall at station A for a certain year, A_a is the annual average at station A, B_y is the total amount of rainfall at station B for a specific year, and B_a is the annual average at station B.

3.4.2 Arithmetic Mean Method

If the usual annual precipitation of the station without the record is within 10% of the normal annual precipitation of the adjacent stations, the missing record is found using the formula below (K.Subramanya, 2005).

$$Px = \frac{1}{M}(P1 + P2 + P3 + \dots + Pn) \dots (2)$$

This procedure is used when the yearly normal precipitation at the station that is close by is more than 10% of the annual normal precipitation at the location where the record is missing (Chaw,1988).

$$Px = \frac{Nx}{M} \left(\frac{P1}{N1} + \frac{P2}{N2} + \dots + \frac{Pm}{Nm} \right) \dots (3)$$

Where, M=number of neighboring stations Pi=annual precipitation at neighboring stations Ni=normal annual precipitation at neighboring stations, Nx=normal annual rain at gauge station x.

3.4.3 Inverse distance weighted

An improved approach is the inverse distance weighted method, which accounts for station distance and specifically varies monthly climate data with distance(Sattari et al., 2017).

$$Px = \frac{\sum_{i=1}^n \frac{Pi}{Di}}{\sum_{i=1}^n \frac{1}{Di}} \dots \dots \dots (4)$$

Where Pi is the amount of precipitation at nearby stations and Di is the distance between stations.

3.5 Different Tests for Rainfall Data

After the rainfall data was gathered, the maximum annual daily rainfall data series was extracted to the corresponding years, the estimation of missing values was done, and the rainfall data quality check was finished, a number of tests were conducted to guarantee the quality of the rainfall data prior to the subsequent steps required to construct IDF curves.

3.5.1 Von-Neumann's Independent Test

The two events are considered independent if there is no connection between the occurrence of one and the other (Xuereb & Green, 2012). This suggests that the following equation gives the joint probability that events A and B would occur equally.

$$\Pr(A \cap B) = \Pr(A) * \Pr(B) \dots (5)$$

P(x) has a value of two if the series X1, X2... Xn are independent and regularly distributed (Haktanir & Citakoglu, 2014).

$$P(x) = \frac{\sum_{i=1}^{n-1} (X_{i+1} - X_i)^2}{\sum_{i=1}^n (X_i - X_{avg})^2} = 2 \dots \dots \dots (6)$$

Where X_{avg} is the series $X_i \dots X_n$ average value.

3.5.2 Evaluating Homogeneity with the Mann-Whitney's Method

This method allows one to confirm that all of the data series' components are derived from the same population and have the same probability distribution (Haktanir & Citakoglu, 2014). This process divides the data series into two ranking sections.

In a manner that $q + p = n, p \leq q$

Next, the value of U will be determined by taking the smaller of V and W, and using the formula below:

$$V = S - \frac{P*(P+1)}{2} \quad W = q * p - V \dots (7)$$

S is the total of the common rankings for both the initial group ranks (p) and the total series (N), which are shown by colors in Chapter 4. The following is the comparison of the values of \bar{U} and Var (U):

$$\bar{U} = \frac{p * q}{2}$$

$$\text{Var}(U) = \left[\frac{P*q}{N*(N-1)} \right] \left[\frac{N^3 - N}{12} \right] + \sum_{i=0}^n T_i \dots (8)$$

$$u = \frac{U - \bar{U}}{\text{var}(U) \left(\frac{1}{2} \right)} \dots \dots \dots (9)$$

Where T_i , refers ties in the groups

The term "ties" in the Mann-Whitney U test describes circumstances in which two or more observations from various groups have the same value. In the event of ties, each tied observation is given its average rank. The anticipated value and variance of U are affected when ties are

present. In these computations, ties are taken into account using specific formulas (Conover, 1981).

3.5.3 Test for Outliers

An outlier is an observation that deviates from the overall rainfall data for a variety of reasons, including mistakes made during data collecting, recording, and measurement, as well as sporadic occurrences from a specific community.

Fitting the distribution to the data becomes challenging as a result of outlier. To test the outliers, one can employ many techniques such as the Z-score method, Box Plot method, Quality control test, Stedinger method, and Grubbs-Beck (G-B) methods. The analysis of rain fall data is affected differently by high and low outliers(Asikoglu, 2017).

3.5.3.1 Grubbs-Beck (G-B) Test

The X_H and X_L values are calculated using the following formulas.

$$X_H = EXP(\bar{X} + KN * S) \dots\dots (10)$$

$$X_L = EXP(\bar{X} - KN * S) \dots\dots\dots (11)$$

Here, \bar{X} and S stand for the sample's natural logarithm mean and standard deviation, respectively, and X_H and X_L , respectively, represent the upper and lower outliers.

KN is calculated using the following formula at a 10% significance level.

$$KN = -3.62201 + 6.28446N^{1/4} - 2.49835N^{1/2} + 0.491436N^{3/4} - 0.037911N \dots (12)$$

Where $5 \leq N \leq 150$ and N=Sample size

Samples with values greater than X_H are considered higher outliers, and samples with values less than X_L are considered lower outliers. Data series that are larger than X_H and smaller than X_L are therefore marked as outlier data (Simeneh Melesse, 2016).

3.6 Disaggregation of Daily Rainfall into Shorter Durations

At intervals of a few minutes, the yearly maximum series is shortened to duration of less than twenty-four hours. There will be a sorting and downscaling of the annual maximum data series into shorter minutes increments(Htun & Thein, 2019).

The sorted yearly maximum data series will be reduced into a time scale of shorter value of less than 24 hours using scoping relationships in the following equation, which was originally proposed by the Indian meteorological agency(Nwaogazie et al., 2021).

$$R_t = R_{24} \left(\frac{t}{24}\right)^n \dots\dots\dots (13)$$

The original meteorological equation from India, with $n = \frac{1}{3}$

R_t = the amount of precipitation needed in millimeters less than a day

t = the necessary amount of time in hours

R_{24} = Rainfall depth per day in millimeters

Chodhury Indian Methodological Department in modified form Equation appeared after the initial equation.

$$R_t = R_{24} \left(\frac{t}{24}\right)^n + C \dots\dots\dots (14)$$

This is how the equation above has been modified.

Where C represents the calibrated constants and n is an exponential(Sam et al., 2023).

3.7 Trend Tests

3.7.1 Mann-Kendall Trend Test

The alternative hypothesis (H_a) and the null hypothesis (H_0) are the foundations of the MK-test, which is used to perform statistically significant rising or falling trends in long span temporal data. Whereas H_a indicates if there is a rising or decreasing trend in the rainfall data, H_0 displays the absence of any trend(Jiqin et al., 2023).

Following is the formula that is given:

$$S = \sum_{i=1}^{n-1} \sum_{k=i+1}^n \text{sign}(X_j - X_i) \dots (15)$$

Where n is the number of data points, and X_j and X_i are the rainfall values for years J and I , respectively, so that

$J > I$ $\text{sign}(X_j - X_i)$ is computed using the formula below.

$$\text{sign}(X_j - X_i) = -1 \text{ for } (X_j - X_i) < 0,$$

$$= 0 \text{ for } (X_j - X_i) = 0,$$

$$= 1 \text{ for } (X_j - X_i) > 0$$

3.8 Generalized Extreme Value Distribution (GEV)

Extreme value analysis commonly makes use of the Generalized Extreme Value Distribution (GEV), a continuous probability distribution function. The distribution of extreme values, such as the highest or lowest value within a set of data, is modeled using this technique (Coles, 2001). The probability density function (PDF) of the GEV distribution is shown in the equation below.

$$f(x) = \frac{1}{\sigma} \left[1 + \xi \left(\frac{x-\mu}{\sigma} \right) \right]^{\left(\frac{-1}{\xi} \right) - 1} * \exp \left[- \left[1 + \xi \left(\frac{x-\mu}{\sigma} \right) \right]^{\left(\frac{-1}{\xi} \right)} \right] \dots (16)$$

The generalized extreme value distribution is the result of combining these three distributions—the Gumbel, Frechet, and Weibull into a single family (Sam et al., 2023). The General extreme value cumulative distribution function $F(x)$ is given by the following equations.

$$F(X) = \exp \left\{ - \left[1 + \frac{\xi(X-\mu)}{\delta} \right]^{-\left(\frac{1}{\xi} \right)} \right\}, \text{ for } \delta > 0, 1 + \frac{\xi(X-\mu)}{\delta} > 0, \xi \neq 0 \dots (17)$$

$$F(x) = \exp \left\{ - \exp \left[- \left(\frac{x-\mu}{\delta} \right) \right] \right\}, \delta > 0, \xi = 0 \dots (18)$$

The shape parameter is represented by ξ , the mean by μ , the standard deviation by σ , the cumulative distribution function by $F(x)$, and the annual extreme value of rainfall by X in this case. The maximum likelihood estimator is the statistical technique used to estimate the distribution parameters since it can be extended to non-stationary evaluation. Three distribution parameters allow for the flexible modeling of various extreme features using the Generalized Extreme Value Distribution. The location parameter (μ) determines the distribution center; the scale parameter (σ) shows the deviation around the location parameter; and the shape parameter (ξ) controls the generalized extreme value distribution's tail behavior.

The shape parameter selects the appropriate distribution type among the three GEV distributions. A value of $\xi=0$ indicates the Gumbel distribution, a value of $\xi<0$ indicates the Weibull distribution, and a value of $\xi>0$ indicates the Frechet distribution (Cheng et al., 2014).

3.8.1 Stationary Generalized Extreme Value Models

Stationary GEV models make the modeling process simpler by assuming that the parameters of the GEV distribution remain constant across time. These models are generally applied to long-term data analysis or any situation where extreme values show signs of stationarity. Using the maximum likelihood estimation method, the parameters of GEV are computed (Coles, 2001).

Table 1: GEV Stationary Parameters Model

GEV Type -0	$\mu(t) = \mu$ $\sigma(t) = \sigma$ $\xi(t) = \xi$	Stationary Parameter model
-------------	--	----------------------------

The location, scale, and shape of the GEV parameters can be described as a contact function by using the maximum likelihood estimator technique.

Under the specified circumstances, the log likelihood function for the stationary case obtained from the equation is as follows:

$$\text{Log } L(\mu, \sigma, \xi | X) = -n * \log \sigma - \left[1 + \frac{1}{\xi} \right] \sum_{i=1}^n \left(\log \left(1 + \xi \left(\frac{x_i - \mu}{\sigma} \right) \right) - \left[\sum_{i=1}^n 1 + \xi \left(\frac{x_i - \mu}{\sigma} \right)^{\frac{1}{\xi}} \right] \right) \quad (19)$$

$$\text{For } \xi \neq 0 \text{ and } 1 + \xi \left(\frac{x_i - \mu}{\sigma} \right) > 0$$

Using this method, the general extreme value distribution parameters in stationary models can be extended to non-stationary models. The maximum likelihood estimator minimizes negative log-likelihood rather than using a straightforward maximization approach.

Given the complexity of the study's equation, R-studio was utilized to fit general extreme parameters based on the stationary model's maximum likelihood estimator to the data. Effectively choosing the best general extreme value model and constructing the rainfall quintile can be done by applying the maximum likelihood estimator approach (Silva et al., 2021).

The general extreme values and the parameters of the extreme distribution will be obtained by an iterative numerical approach by minimizing the negative log-likelihood function.

3.9 Development of GEV Intensity Duration Frequency Curves

Rainfall intensity duration frequency curves were created in this study using R-studio software. Estimating precipitation intensities using the model parameters involves applying the GEV distribution return periods and return levels of extremes, as well as formulating the function of return level as the return period.

$$T = \frac{1}{1-p} \dots \dots \dots (20)$$

$$T = \frac{1}{q} \dots \dots \dots (21)$$

p is the non-exceedance probability and q is the exceedance probability of occurrence in a given year, as it is regarded as constant in the stationary model. The intensity of the stationary rainfall extreme value is computed using the following formula(Silva et al., 2021).

$$X_T = \mu - \frac{\sigma}{\xi} [1 - \{-\ln(1 - \frac{1}{T})\}^{-\xi}] \quad \text{for } \xi \neq 0 \dots \dots \dots (22)$$

T represents the return period, while XT is the degree of rainfall intensity exceedance.

CHAPTER 4: RESULTS AND DESCUSSION

4.1 Preparation of Rainfall Data

The National Metrological Agency of Ethiopia provided the study with the rainfall data, which were chosen based on a variety of factors, including the duration of the record year and hydrological tests that more accurately reflected the rainfall characteristics of the study area.

In addition to having automatically recorded rainfall values that were used for calibration and validation, four nearby rainfall stations Meshenti Rainfall Station, Bahir Dar Airport Station, Tisabay, and Debre Markos Station that have better record lengths were used in this study. Other stations, despite being close to the study area, do not have automatically recorded rainfall values.

4.1.1 Filling of the Missing Rainfall Data

It was found that different months had varying numbers of missed values at the Debre Markos rainfall station over a 43-year period (1980–2022), hence it was necessary to take certain filling techniques into consideration in order to obtain adequate missed values.

For a few years, the daily rainfall data statistics contained missing numbers. The overall missing value within the forty-three-year rainfall record was calculated by adding the monthly missed values, which were counted using an Excel code for each corresponding year.

Total value of data within 43 years =15738

Leap year means additional day per four years

Total missed value within 43 years =588

Leap years=11

$$\text{Percent of Missing} = \left(\frac{588}{15749} \right) * 100 = 3.73 \% < 10\%$$

Since $3.73 < 10$, the missing rainfall amounts were filled in using the simple arithmetic mean technique of data filling. This shows that while 96% of the rainfall data were available, 3.73 percent of the rainfall data were these lost numbers. 2020 had the most missed value, accounting for 72.79% of all missed values. The year 1991 had the next-highest missing value, accounting for 18.37% of the overall missed value, while the year 1980 had the lowest proportion, accounting for 0.51% of the total missed value.

4.1.2 Arithmetic Mean Method

The missing record is determined using the following formula if the typical annual precipitation of the nearby station is within 10% of the normal annual precipitation of the station lacking a record (K.Subramanya, 2005).

$$P_x = \frac{1}{M} (P_1 + P_2 + P_3 + \dots + P_m)$$

Whereas P_i is the annual precipitation at the nearby station. M =number of precipitation

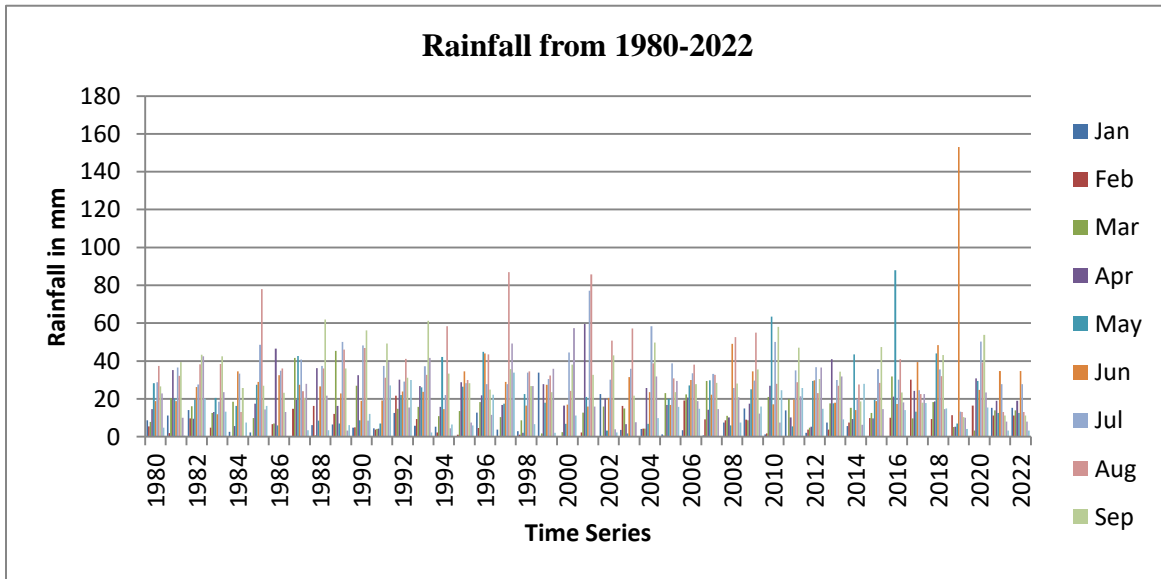


Figure 2: Debre Markos Rainfall Station Rainfall Data Time Series

4.2 Different Tests for Debre Markos Station Rainfall Data

Various tests were conducted to examine the impact of various factors on the subsequent steps till the development of IDF curves, following the sorting of the maximum annual daily rainfall data series of all years.

4.2.1 Von-Neumann's Independent Test

The function $P(x)$ has a value of two if the series X_1, X_2, \dots, X_n are independent and regularly distributed (Haktanir & Citakoglu, 2014).

$$P(x) = \frac{\sum_{i=1}^{n-1} (X_{i+1} - X_i)^2}{\sum_{i=1}^n (X_i - X_{avg})^2} = 2$$

Where X_{avg} is the series' average value $X_1 \dots X_n$

Table 2: Von-Neumann's Independent Test

Year	Max RF	Arithmetic Mean	$(X_i - X_{avg})^2$	$(X_{i+1} - X_i)^2$
1980	37.40	52.18	218.45	4.00
1981	39.40	52.18	163.33	16.00
1982	43.40	52.18	77.08	0.81
1983	42.50	52.18	93.70	64.00
1984	34.50	52.18	312.58	1892.25
1985	78.00	52.18	666.67	985.96
1986	46.60	52.18	31.13	16.00
1987	42.60	52.18	91.78	376.36
1988	62.00	52.18	96.43	144.00
1989	50.00	52.18	4.75	37.21
1990	56.10	52.18	15.37	47.61
1991	49.20	52.18	8.88	65.61
1992	41.10	52.18	122.77	408.04
1993	61.30	52.18	83.17	8.41
1994	58.40	52.18	38.69	566.44
1995	34.60	52.18	309.06	104.04
1996	44.80	52.18	54.46	1772.41
1997	86.90	52.18	1205.47	2745.76
1998	34.50	52.18	312.58	1.96
1999	35.90	52.18	265.03	457.96
2000	57.30	52.18	26.21	806.56
2001	85.70	52.18	1123.59	1225.00
2002	50.70	52.18	2.19	40.96
2003	57.10	52.18	24.21	1.44
2004	58.30	52.18	37.45	384.16
2005	38.70	52.18	181.71	0.49
2006	38.00	52.18	201.07	24.01
2007	33.10	52.18	364.05	77.44
2008	41.90	52.18	105.68	114.49
2009	52.60	52.18	0.18	5.76
2010	55.00	52.18	7.95	72.25
2011	63.50	52.18	128.14	272.25
2012	47.00	52.18	26.83	106.09
2013	36.70	52.18	239.63	18.49
2014	41.00	52.18	124.99	6.25
2015	43.50	52.18	75.34	14.44

2016	47.30	52.18	23.81	1656.49
2017	88.00	52.18	1283.07	2361.96
2018	39.40	52.18	163.32	81.00
2019	48.40	52.18	14.29	10951.23
2020	153.05	52.18	10174.76	9850.19
2021	53.80	52.18	2.62	364.81
2022	34.70	52.18	305.55	
Sum			18807.71	38150.60
			P(x)	2.0

$$P(x) = \frac{38150.60}{18807.71} = 2.0$$

Given that it met Von-Neumann's formula requirements $P(x) = \frac{\sum_{i=1}^{n-1} (X_{i+1} - X_i)^2}{\sum_{i=1}^n (X_i - X_{avg})^2} = 2$

The rainfall data is found to be independent.

4.2.2 Testing for Homogeneity using Mann-Whitney's Method

Using this method, one can confirm that each element of the data series comes from the same population and has the same probability distribution (Haktanir & Citakoglu, 2014). With this method, the data series is split into two groups based on rankings.

In a way that $q + p = n, p \leq q$

The value of U and other required values are then computed using the following formula in order to compare u with $P_{Critical}$, the smaller value, V or W:

$$V = S - \frac{P*(P+1)}{2} \quad W = q * p - V$$

$$\bar{U} = \frac{p * q}{2}$$

$$\text{Var}(U) = \left[\frac{P * q}{N * (N - 1)} \right] \left[\frac{N^3 - N}{12} \right] + \sum_{l=0}^n T$$

$$u = \frac{u - \bar{U}}{\text{var}(U) \left(\frac{1}{2} \right)}$$

Table 3: Mann-Whitney's Homogeneity Test

P	Annual Max daily RF	q	Annual Max daily RF	N=P+q	Annual Max daily RF
1	37.40	1	85.70	1	33.10
2	39.40	2	50.70	2	34.50
3	43.40	3	57.10	3	34.50
4	42.50	4	58.30	4	34.60
5	34.50	5	38.70	5	34.70
6	78.00	6	38.00	6	35.90
7	46.60	7	33.10	7	36.70
8	42.60	8	41.90	8	37.40
9	62.00	9	52.60	9	38.00
10	50.00	10	55.00	10	38.70
11	56.10	11	63.50	11	39.40
12	49.20	12	47.00	12	39.40
13	41.10	13	36.70	13	41.00
14	61.30	14	41.00	14	41.10
15	58.40	15	43.50	15	41.90
16	34.60	16	47.30	16	42.50
17	44.80	17	88.00	17	42.60
18	86.90	18	39.40	18	43.40
19	34.50	19	48.40	19	43.50
20	35.90	20	153.05	20	44.80
21	57.30	21	53.80	21	46.60
		22	34.70	22	47.00
				23	47.30
				24	48.40
				25	49.20
				26	50.00
				27	50.70
				28	52.60
				29	53.80
				30	55.00
				31	56.10
				32	57.10
				33	57.30
				34	58.30
				35	58.40
				36	61.30
				37	62.00
				38	63.50
				39	78.00

	40	85.70
	41	86.90
	42	88.00
	43	153.05

The following step was determining the value of S after splitting the data series into two ordered groups, such as p=21 and q=22, and sorting the entire series in decreasing order.

$$S = 2 + 3 + 4 + 6 + 8 + 12 + 14 + 16 + 17 + 18 + 20 + 21 + 25 + 26 + 31 + 33 + 35 \\ + 36 + 37 + 39 + 41 = 444$$

S = Total of common rankings for the initial group ranks (p) and the overall series (N) that are colored-highlighted. The competition for the values of V and W is as follows:

$$V = S - \frac{P * (P + 1)}{2}$$

$$V = 444 - \frac{21*(21+1)}{2} = 444 - 231 = 213$$

And the W value determined using the following formula:

$$W = q * p - V$$

$$W = 21 * 22 - 212 = 462 - 213 = 249$$

U is equal to the smaller of V or W.

$$U=213$$

$$\bar{U} = \frac{p*q}{2} = \frac{21*22}{2} = 231$$

$$\text{Var}(U) = \left[\frac{P * q}{N * (N - 1)} \right] \left[\frac{N^3 - N}{12} \right] + \sum_{l=0}^n T$$

Where T, refers ties in the groups

$$\sum_{l=1}^{43} T=0$$

$$\text{Var}(U) = \left[\frac{21 * 22}{43 * (43 - 1)} \right] \left[\frac{43^3 - 43}{12} \right] + \sum_{l=1}^{43} 0$$

$$\text{Var}(U) = 0.256 * 6622 + \sum_{l=1}^n 0 = 1694$$

$$\text{Var}(U) = 1694$$

Finally the parameter, u is computed using the formula

$$u = \frac{u - \bar{U}}{\text{var}(U)^{\frac{1}{2}}}$$

$$u = \frac{213 - 231}{(1694)^{\frac{1}{2}}} = -0.44$$

A	5%
1-a/2	0.975
P _{Critical}	1.959964

$|u| = 0.44 \leq 1.96$ the crucial value, indicating homogeneity at the 5% significance level for the yearly daily maximum rainfall

4.2.3 Test for Outliers

4.2.3.1 Grubbs-Beck (G-B) Test

An observation of rainfall that differs from the rest of the data for any number of reasons is called an outlier. The X_H and X_L values are calculated using the following formulas.

$$X_H = \text{EXP}(\bar{X} + KN * S)$$

$$X_L = \text{EXP}(\bar{X} - KN * S)$$

Where X_H and X_L are the upper and lower outliers, respectively, and \bar{X} and S are the sample's natural logarithms of the mean and standard deviations, respectively. The following formula determines KN at a 10% significant level.

$$K_N = -3.62201 + 6.28446N^{1/4} - 2.49835N^{1/2} + 0.491436N^{3/4} - 0.037911N$$

Where N =Sample size and $5 \leq N \leq 150$ in this thesis case for 1st station $N=43$

Those in the sample that fall below X_L are considered lower outliers, whereas those that are higher than X_H are considered high outliers. Data series that are larger than X_H and smaller than X_L are therefore marked as outlier data.

$$KN = -3.62201 + 6.28446 * 43^{\frac{1}{4}} - 2.49835 * 43^{\frac{1}{2}} + 0.491436 * 43^{\frac{3}{4}} - 0.037911 * 43$$

$$K_N = 24.11 - 21.17 = 2.94$$

$$K_N = 2.71$$

The computation of the upper and lower bounds comes next.

Table 4: Debre Markos Rainfall Station Rainfall Grubbs-Beck Outlier Test

Year	R=Max Annual Daily RF	lnR	Mean of lnR	St. deviation lnR
1980	37.4	3.62	3.90	0.313
1981	39.40	3.67	3.90	0.313
1982	43.40	3.77	3.90	0.313
1983	42.50	3.75	3.90	0.313
1984	34.50	3.54	3.90	0.13
1985	78.00	4.36	3.90	0.313
1986	46.60	3.84	3.90	0.313
1987	42.60	3.75	3.90	0.313
1988	62.00	4.13	3.90	0.313
1989	50.00	3.91	3.90	0.313

1990	56.10	4.03	3.90	0.313
1991	49.20	3.90	3.90	0.313
1992	41.10	3.72	3.90	0.313
1993	61.30	4.12	3.90	0.313
1994	58.40	4.07	3.90	0.313
1995	34.60	3.54	3.90	0.313
1996	44.80	3.80	3.90	0.313
1997	86.90	4.46	3.90	0.313
1998	34.50	3.54	3.90	0.313
1999	35.90	3.58	3.90	0.313
2000	57.30	4.05	3.90	0.313
2001	85.70	4.45	3.90	0.313
2002	50.70	3.93	3.90	0.313
2003	57.10	4.04	3.90	0.313
2004	58.30	4.07	3.90	0.313
2005	38.70	3.66	3.90	0.313
2006	38.00	3.64	3.90	0.313
2007	33.10	3.50	3.90	0.313
2008	41.90	3.74	3.90	0.313

2009	52.60	3.96	3.90	0.313
2010	55.00	4.01	3.90	0.313
2011	63.50	4.15	3.90	0.313
2012	47.00	3.85	3.90	0.313
2013	36.70	3.60	3.90	0.313
2014	41.00	3.71	3.90	0.313
2015	43.50	3.77	3.90	0.313
2016	47.30	3.86	3.90	0.313
2017	88.00	4.48	3.90	0.313
2018	39.40	3.67	3.90	0.313
2019	48.40	3.88	3.90	0.313
2020	153.05	5.03	3.90	0.313
2021	53.80	3.99	3.90	0.313
2022	34.70	3.55	3.90	0.313
			Mean lnR=3.90	St.deviation.S=0.313

The next stage after calculating statistical parameters is to establish upper and lower bounds.

$$K_N=2.71$$

Upper Limit

$$X_H = EXP(\bar{X} + KN * S)$$

$$X_H = EXP(3.90 + 2.71 * 0.313)$$

$$X_H = EXP(4.748) = \mathbf{115.38 \text{ mm}}$$

Lower

$$X_L = EXP(\bar{X} - KN * S)$$

$$X_L = EXP(3.90 - 2.71 * 0.313)$$

$$X_L = EXP(3.052) = \mathbf{21.53mm}$$

The findings indicate that, in terms of annual maximum daily rainfall data, the lowest value is 21.53 mm and the highest value is 115.38 mm. This suggests that values falling outside of these ranges need to be carefully examined. For instance, the figure 153.05 in 2020 falls outside of this range, indicating that a flood with a rainfall depth of 153.05 mm occurred. However, no value was found to be smaller than 21.53mm.

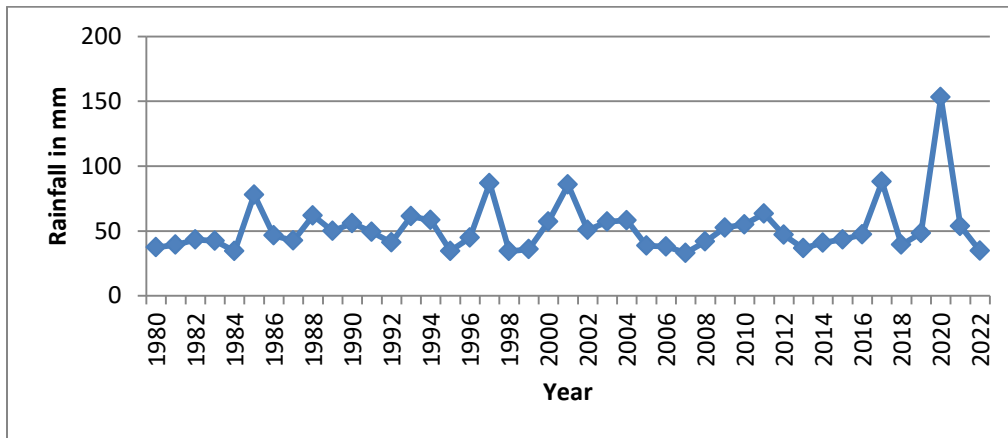


Figure 3: Debre Markos Rainfall Station Rainfall Data Outlier Plot

4.3 Disaggregation of Daily Rainfall Data into Shorter Durations

Four stations of Tisabay, Bahir Dar Airport, Meshenti (1982-2022) and Debre Markos (1980-2022) rainfall data were used to conduct this thesis work. For instance Meshenti station's 41 years of annual maximum daily rainfall data series sorted out were disaggregated into shorter duration's of 10 minutes, 15 minutes, 30 minutes, 45 minutes, 60 minutes (1hr), 120 minutes (2hr), and 180 minutes (3hr). Secondly Debre Markos's 43 years of annual maximum daily rainfall data series sorted out were also downscaled into shorter durations of 15 minute ,30 minute ,45 minute ,60 minute ,120 minutes ,and 180 minutes.

Comparable work was completed for the remaining rainfall stations. The following equation, which was originally intended by the Indian Methodological Department, was used to reduce the sorted annual maximum daily rainfall values into time scales of 24 hours and shorter durations. After calibration

$$R_t = R_{24} \left(\frac{t}{24}\right)^n$$

The original Indian meteorological formula, which $n = \frac{1}{3}$

R_t = The millimeter-wise required rainfall depth in less than a day

t = the required amount of time in hours

R_{24} = daily rainfall depth in millimeters

Chodhury Indian Methodological Department, amended Equation followed the first equation in appearance.

$$R_t = R_{24} \left(\frac{t}{24}\right)^n + C \dots \dots \dots (3)$$

It is the equation mentioned above modified. Where C represents the calibrated constants and n is an exponential. The upgraded Chodhury Indian Methodological Department made the changes. Formula (Nwaogazie et al., 2021).

4.4 Calibration

Using an Excel solver, the modified Chodhury Indian methodological department equation was calibrated. The GEV IDF curves for the research area are derived from the actual observed rainfall or the rainfall utilized to construct the control experiment. The three years of disaggregated rainfall values utilizing the first Indian methodological department equation were compared with the three years of actual observed rainfall values (2016–2018). The process of optimization involved minimizing the sum of square differences between the rainfall values that were produced by downscaling and the actual rainfall values that were observed.

The Chodhury Indian methodological department Equation was adjusted, and the optimization function was carried out until the best value of the constant C and the exponent n was reached. Following multiple calibrations, the n power coefficient in this study was found to be 0.24, and

the constant C was 11. The equation above is changed to: once the constant C of 11 and the coefficient values of 0.24 are added.

$$R_t = R_{24} \left(\frac{t}{24}\right)^{0.24} + 11 \dots \dots (4)$$

By repeatedly changing the values of n and C, the total was lowered. The goal is to reduce the gap between the calculated and observed values in order to get a reduced total of square differences. The yearly daily maximum rainfall was downscaled to shorter durations for the corresponding processes after calibration.

Table 5: Debre Markos Station Rainfall Annual Maximum Disaggregated Rainfall

Year	AMS	15min	30 min	45 min	60 min	120min	180 min
1980	37.4	23.51	25.77	27.28	28.44	31.60	33.71
1981	39.4	24.18	26.56	28.15	29.38	32.70	34.92
1982	43.4	25.51	28.14	29.89	31.24	34.90	37.35
1983	42.5	25.21	27.78	29.50	30.82	34.41	36.80
1984	34.5	22.54	24.62	26.02	27.09	30.00	31.94
1985	78	37.08	41.80	44.95	47.38	53.96	58.35
1986	46.6	26.58	29.40	31.28	32.73	36.67	39.29
1987	42.6	25.25	27.82	29.54	30.87	34.46	36.86
1988	62	31.73	35.48	37.99	39.92	45.15	48.64
1989	50	27.72	30.75	32.76	34.32	38.54	41.35
1990	56.1	29.76	33.15	35.42	37.16	41.90	45.06
1991	49.2	27.45	30.43	32.42	33.95	38.10	40.87
1992	41.1	24.74	27.23	28.89	30.17	33.64	35.95
1993	61.3	31.50	35.21	37.68	39.59	44.76	48.22
1994	58.4	30.53	34.06	36.42	38.24	43.17	46.45

1995	34.6	22.57	24.66	26.06	27.14	30.06	32.01
1996	44.8	25.98	28.69	30.50	31.89	35.68	38.20
1997	86.9	40.06	45.32	48.83	51.53	58.86	63.76
1998	34.5	22.54	24.62	26.02	27.09	30.00	31.94
1999	35.9	23.00	25.18	26.63	27.74	30.77	32.79
2000	57.3	30.16	33.63	35.94	37.72	42.56	45.79
2001	85.7	39.66	44.84	48.30	50.97	58.20	63.03
2002	50.7	27.95	31.02	33.07	34.65	38.93	41.78
2003	57.1	30.09	33.55	35.85	37.63	42.45	45.67
2004	58.3	30.50	34.02	36.38	38.19	43.11	46.39
2005	38.7	23.94	26.28	27.85	29.05	32.32	34.49
2006	38	23.71	26.01	27.54	28.72	31.93	34.07
2007	33.1	22.07	24.07	25.41	26.44	29.23	31.09
2008	41.9	25.01	27.55	29.24	30.54	34.08	36.44
2009	52.6	28.59	31.77	33.90	35.53	39.97	42.93
2010	55	29.39	32.72	34.94	36.65	41.29	44.39
2011	63.5	32.23	36.08	38.64	40.62	45.98	49.55
2012	47	26.72	29.56	31.46	32.92	36.89	39.53
2013	36.7	23.27	25.49	26.97	28.12	31.21	33.28
2014	41	24.71	27.19	28.85	30.12	33.58	35.89
2015	43.5	25.55	28.18	29.93	31.29	34.96	37.41
2016	47.3	26.82	29.68	31.59	33.06	37.05	39.72
2017	88	40.43	45.75	49.30	52.04	59.47	64.42
2018	39.4	24.18	26.56	28.15	29.38	32.70	34.92

2019	48.4	27.18	30.11	32.07	33.57	37.66	40.38
2020	153.05	33.43	42.11	48.21	53.06	66.85	76.55
2021	53.8	28.99	32.25	34.42	36.09	40.63	43.66
2022	34.7	22.60	24.70	26.10	27.18	30.11	32.07

The updated Chodhury Indian methodological department Equation indicates that the rainfall depths have higher values than the Indian methodological department's first disaggregation, which causes an increase in intensity.

4.5 Trend Test

4.5.1 Mann-Kendall Trend Test

The MK-test is used to perform statistically significant rising or decreasing patterns in long-term temporal data based on two hypotheses: the alternative hypothesis (Ha) and null hypothesis (Ho). In the rainfall data, Ho indicates that there is no trend, whereas Ha communicates that there is an increasing or declining trend (Jiqin et al., 2023).

Following is the formula that is given:

$$S = \sum_{i=1}^{n-1} \sum_{k=i+1}^n \text{sign}(X_j - X_i)$$

S is a number's related positive or negative value.

Where X_j and X_i are the rainfall values in J and I years, and n is the number of data points.

$J > I$. $\text{sign}(X_j - X_i)$ Is calculated by the equation under here

$$\text{sign}(X_j - X_i) = -1 \text{ for } (X_j - X_i) < 0,$$

$$0 \text{ for } (X_j - X_i) = 0,$$

$$1 \text{ for } (X_j - X_i) > 0$$

Σ sign is computed in this study using logical Excel codes, and the findings are presented in the table below.

Table 6: Man-Kendall Trend Test

Year	Annual Maximum Daily Rainfall	Rank	Σ sign
1980	48.40	8	27
1981	50.40	11	21
1982	54.40	18	9
1983	53.50	16	12
1984	45.50	2	34
1985	89.00	39	-30
1986	57.60	21	5
1987	53.60	17	10
1988	73.00	37	-25
1989	61.00	26	-4
1990	67.10	31	-13
1991	60.20	25	-4
1992	52.10	14	9
1993	72.30	36	-20
1994	69.40	35	-19
1995	45.60	4	22
1996	55.80	20	3
1997	97.90	41	-22
1998	45.50	2	21
1999	46.90	6	18

2000	68.30	33	-13
2001	96.70	40	-18
2002	61.70	27	-5
2003	68.10	32	-12
2004	69.30	34	-13
2005	49.70	10	8
2006	49.00	9	9
2007	44.10	1	14
2008	52.90	15	5
2009	63.60	28	-4
2010	66.00	30	-7
2011	74.50	38	-8
2012	58.00	22	-1
2013	47.70	7	6
2014	52.00	13	3
2015	54.50	19	2
2016	58.30	23	1
2017	99.00	42	-4
2018	50.40	11	1
2019	59.40	24	0
2020	153.05	43	1
2021	64.80	29	-2
2022	45.7	5	0

Additional MK parameters can be computed using the table above.

$$N=43, N-1=42$$

$$S = \sum_{i=1}^{n-1} \sum_{k=2}^n \text{sign} = 13$$

$$\text{Var}(S) = 9130.333333 = N * (N - 1) * \frac{(2N+5)}{18}$$

$$Z_{\text{statistical}} = \frac{|S|}{\sqrt{\text{var}(S)}}$$

$$Z_{\text{statistical}} = 0.136050467$$

At significant level $\alpha = 5\%$

Normal distribution value $= 1 - \frac{\alpha}{2} = 1 - \frac{5\%}{2} = 0.975$ using this result excel calculated the critical Z value.

$$Z_{\text{critical}} = 1.959963985$$

There is no trend in the data and that employing a stationary model rather than a non-stationary model is supported by the fact that the Z statistics is smaller than the Z_{critical} .

4.5.2 R-Studio Trend Sample Test Results for Different Stations

`mk.test (Meshenti_for_R$Min_30)`

Mann-Kendall trend test

```

Data: Meshenti_for_R$Min_30
z = 1.037, n = 35, p-value = 0.2997
alternative hypothesis: true S is not equal to 0
sample estimates:
      S      varS      tau
74.0000000 4955.3333333 0.1246845

```

`mk.test (Bahir_Dar_main_forR$Min_180)`

Mann-Kendall trend test

```

data: Bahir_Dar_main_for R$Min_180
z = 1.257, n = 31, p-value = 0.3456
alternative hypothesis: true S is not equal to 0
sample estimates:
      S      varS      tau
76.0000000 3455.167873 0.1267845

```

As seen from the above RStudio results, **z-statistical value = 1.037 < z-value critical = 1.959963985** and **zstatistical = 1.257 < z-value critical = 1.959963985** for two cases there is no trend in two stations this is critical evidence for using GEV stationary model for calculating distribution and return levels.

4.6 Deriving Two, Three and Five Days Rainfall from Annual Maximum Daily Rainfall

In order to develop IDF curves for two, three and five days it must be mandatory to derive rainfall from previous day for each day first. There are certain methods to estimate data for future use from the previous data such as rolling aggregation and Moving average methods

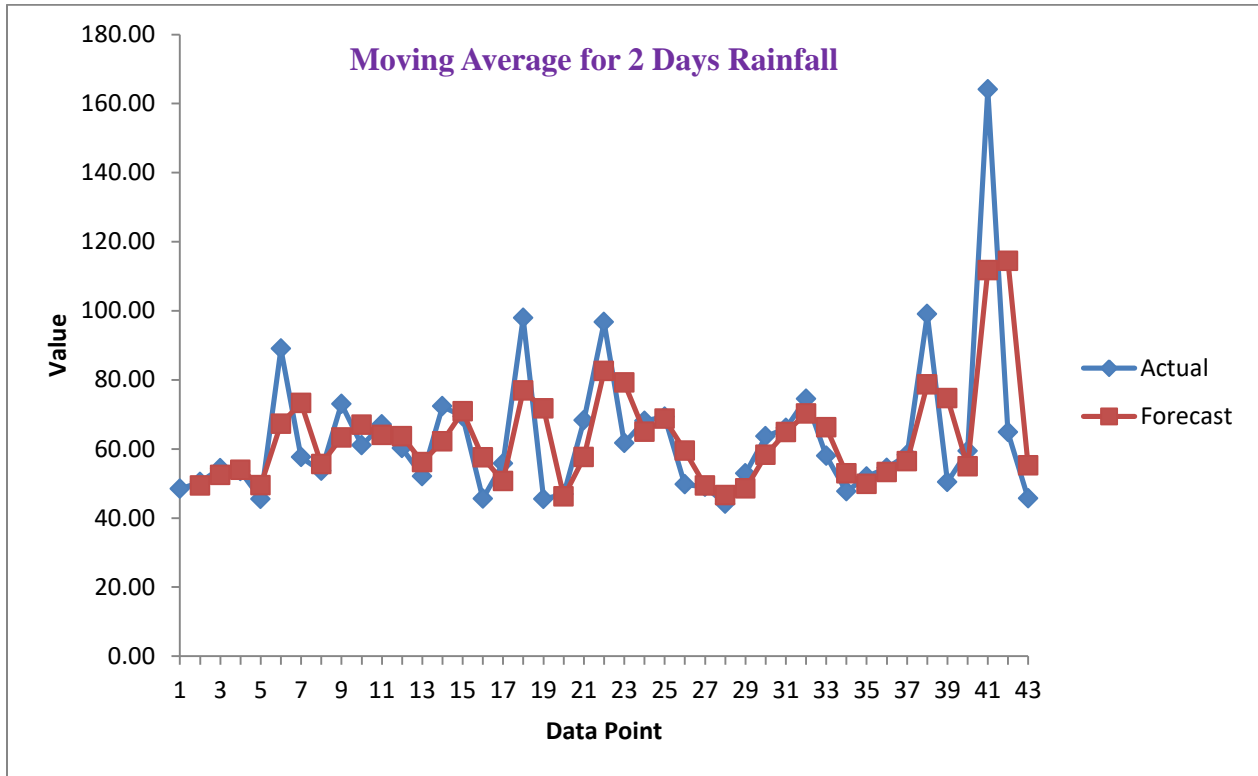
The Moving average method was used to derive two ,three and five days rainfall data from daily rainfall data because it is easy to apply, good to handle outliers, enable to calculate future values from previous values. It calculates the unknown values by taking sum of two, three and five day's consecutive values and divide the sum by Two,Three,and five respectively.

Table 7: Deriving Debre Markos Rainfall Station's Two, Three, and Five Days Rainfall from Annual Maximum Daily Rainfall

Day_1	Day_2	Day_3	Day_5
48.40	#N/A	#N/A	#N/A
50.40	49.40	#N/A	#N/A
54.40	52.40	51.07	#N/A
53.50	53.95	52.77	#N/A
45.50	49.50	51.13	50.44
89.00	67.25	62.67	58.56
57.60	73.30	64.03	60.00
53.60	55.60	66.73	59.84
73.00	63.30	61.40	63.74
61.00	67.00	62.53	66.84
67.10	64.05	67.03	62.46
60.20	63.65	62.77	62.98
52.10	56.15	59.80	62.68
72.30	62.20	61.53	62.54
69.40	70.85	64.60	64.22

45.60	57.50	62.43	59.92
55.80	50.70	56.93	59.04
97.90	76.85	66.43	68.20
45.50	71.70	66.40	62.84
46.90	46.20	63.43	58.34
68.30	57.60	53.57	62.88
96.70	82.50	70.63	71.06
61.70	79.20	75.57	63.82
68.10	64.90	75.50	68.34
69.30	68.70	66.37	72.82
49.70	59.50	62.37	69.10
49.00	49.35	56.00	59.56
44.10	46.55	47.60	56.04
52.90	48.50	48.67	53.00
63.60	58.25	53.53	51.86
66.00	64.80	60.83	55.12
74.50	70.25	68.03	60.22
58.00	66.25	66.17	63.00
47.70	52.85	60.07	61.96
52.00	49.85	52.57	59.64
54.50	53.25	51.40	57.34
58.30	56.40	54.93	54.10
99.00	78.65	70.60	62.30
50.40	74.70	69.23	62.84

59.40	54.90	69.60	64.32
164.05	111.72	91.28	86.23
64.80	114.42	96.08	87.53
45.70	55.25	91.52	76.87



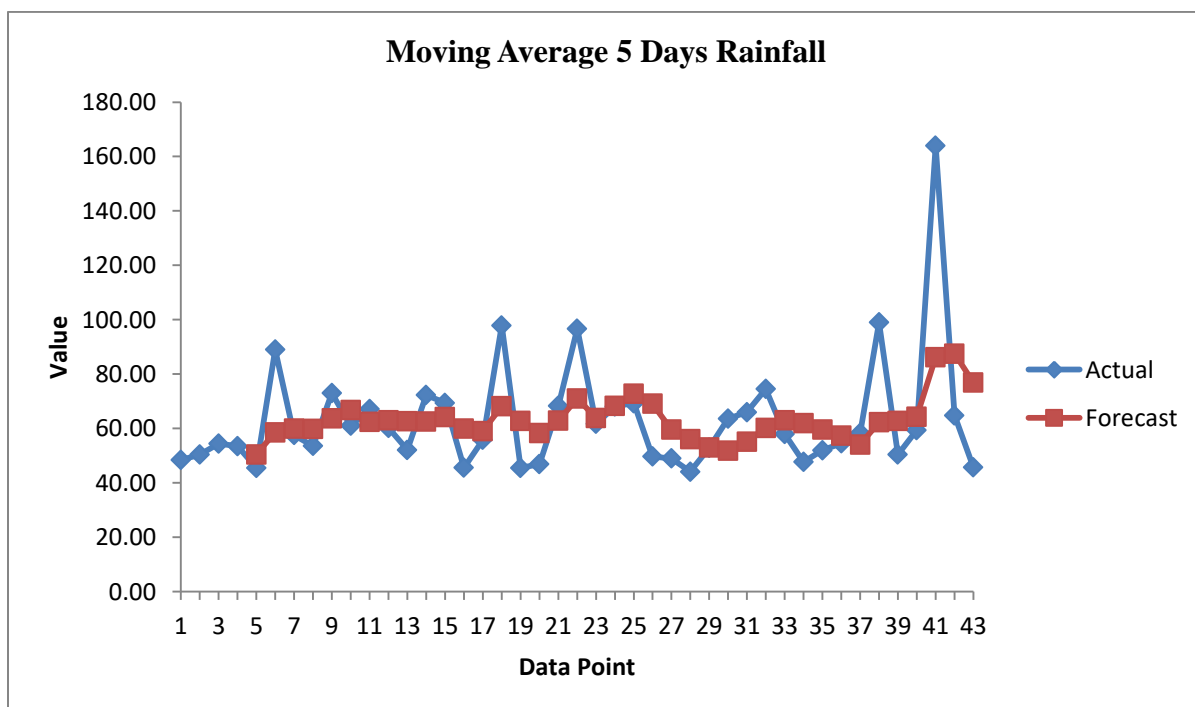
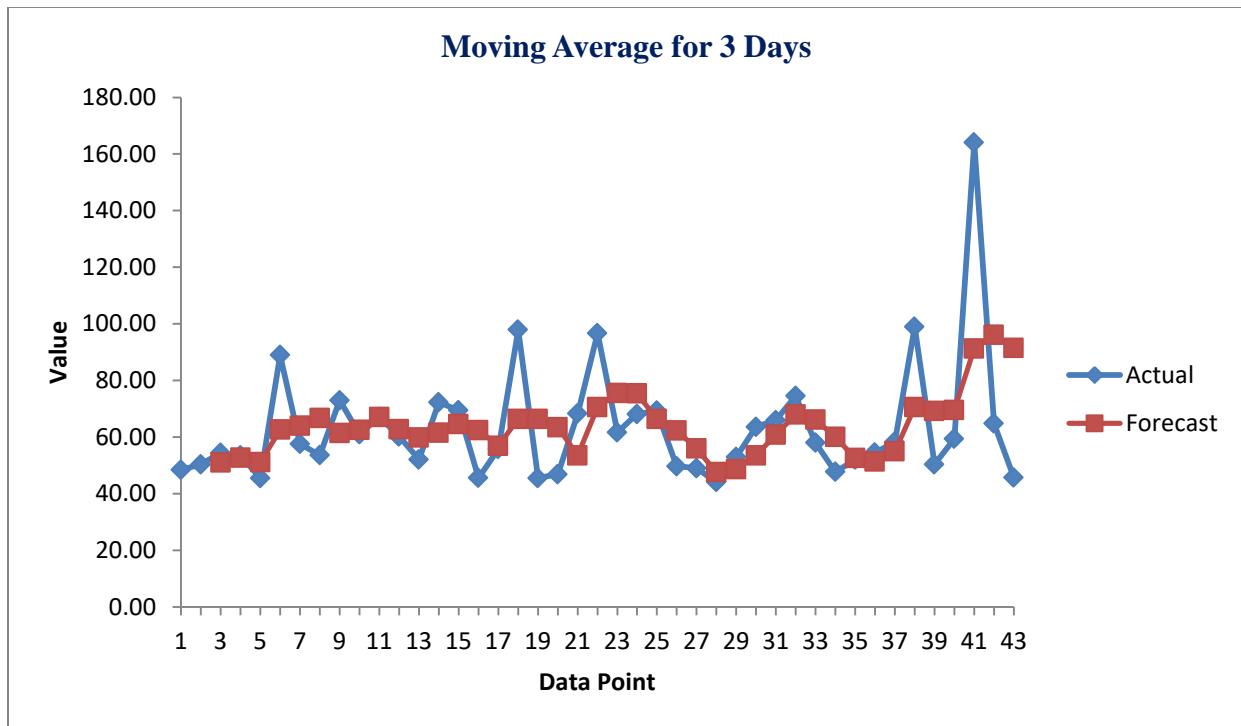


Figure 4: Moving Average Plots for Debre Markos Rainfall Station

The two and the three days moving averages are predicted the future values in the better way because as seen from the plot the moving average changes quickly based on the previous days

while the moving average for five days is smoother it didn't change a lot. The two and three days moving averages have smaller standard errors than the five days standard error.

4.7 Evaluation of Parameter Model Comparing Criteria

The statistical technique used to calculate the distribution parameters is called the maximum likelihood estimator. The R-Studio program was used to integrate pertinent functions with corresponding packages in order to estimate different parameters.

The parameters of the GEV distribution were estimated using the maximum likelihood estimator approach. The parameters of a stationary model are not affected by time, but the parameters of non-stationary models are affected by time and exhibit time-varying features.

Therefore it is possible to conclude that all MO models for each duration and return years are stationary; all are used for computing their respective return levels and the rest of other are non-stationary because all parameters are dependent of time. For stationary model, the GEV Type-0 for all respective duration is taken.

To identify which model was the best despite being non-stationary, one can also use the statistical method known as the corrected Akaike's information criterion (AICC), in addition to AIC and BIC. The following formulas were used in the process:

$$AIC = -2\log L + 2K$$

$$AICc = AIC(k) + \frac{2k(k+1)}{n-k-1}$$

$$BIC = K * \ln(n) - 2 * \ln(L)$$

Where k represents all of the parameters in a particular model(Silva et al., 2021). For this research, calculations were made for each model durations using the equations mentioned above. However, in the case of the stationary model, it became necessary to compute return levels for all stationary models using the representative of all durations.

Using RStudio software, the next step is to estimate the intensity or return levels of rainfall based on the stationary and non-stationary model equations.

4.8 Evaluation of Time-Variat Parameter

A process is considered stationary when statistical properties such as mean, variance, and auto covariance do not change over time. Trends, seasonality, and other time-varying characteristics are displayed by the non-stationary processes. In these situations, the non-stationary behavior was analyzed using more sophisticated models. Model equations for trend models are commonly used in non-stationary procedures. The characteristics of the data being examined influence the model equation selection. To choose the best fit model, information criteria like AIC and BIC were taken into consideration, along with diagnostic tests, autocorrelations, and partial autocorrelation functions. As a result, the non-stationary is represented by adding one or more GEV distribution parameters as a function of time.

4.9 Goodness of Fit Test

Using a graphical diagnostic test to determine which GEV distribution model best fits the sample rainfall data would be a useful endeavor. The distribution can be fitted using a variety of graphical and numerical techniques; the degree to which the fitted model fits the sample data should be assessed based on the models and functions that were employed.

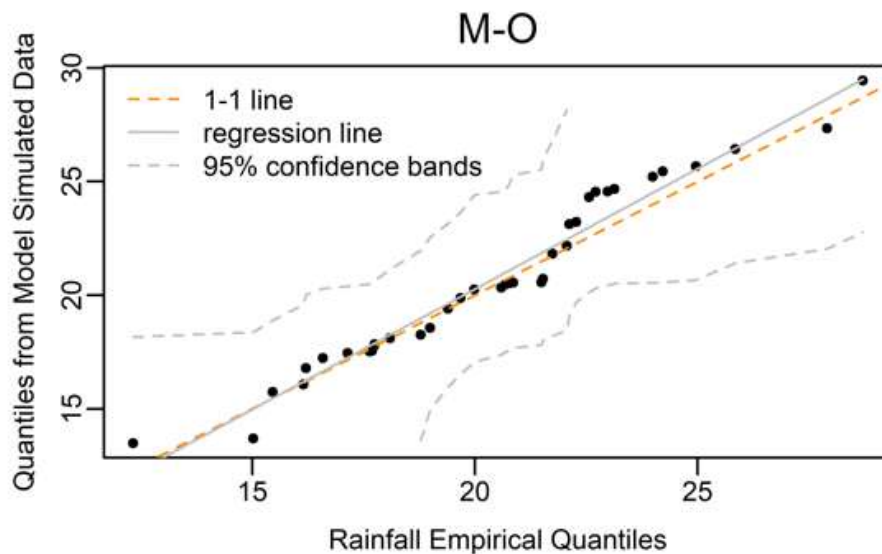


Figure 5: Sample Rainfall Quantile Plot for 10 Minutes Duration

If every scatter follows the 1-1 axis, a better match is assured as seen by the graphical diagnosis plotted above. The model's Q-Q plot was also used to assess how well the model fit; in model M-0, the scatters appear to follow the 1-1 line quite well, whereas in model A, the scatters fall between the upper and lower bounds of the 95% confidence band. There is also a closer relationship between the regression line and the 1-1 line. The return levels for each time frame of the return periods of 2, 5, 10, 25, 50, and 100 years were predicted using the parameters of the best-fit GEV model.

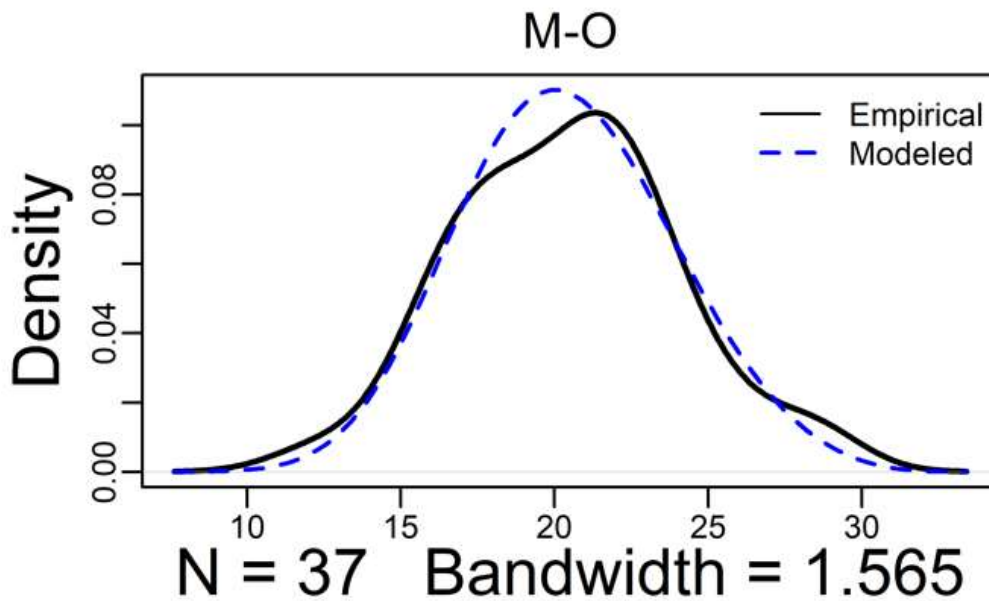


Figure 6: Sample Density Plot for Simulated and Fitted Rainfall Data

The model simulation plot and the rain fall sample fitted to the GEV stationary distribution are displayed in the above figure. For these reasons, M-0 is the best fit stationary model to the sample rainfall data. The figure in the density plot indicates that the model M-0 appeared to be similar in shape to the fitted sample (empirical) rainfall data. Similarly, the regression line of M-0 converged to 1-1 line in the quantile line plot of the stationary model. The aforementioned figures demonstrate that the best fitting model to the sample rainfall data is M-0, since it fits the data better and has a shape that is close to the observed rainfall data.

4.10 Development of GEV Stationary Models IDF Curves

Careful data analysis, statistical modeling, or consideration of changing rainfall event features over time were necessary for the construction of GEV-based IDF curves, whether stationary or non-stationary models. These curves will offer important data for infrastructure design, flood risk assessment, and managing water resources in the face of shifting climate circumstances.

The closest rainfall station in Merawi Town provided rainfall data records for a considerable amount of time. From the rainfall data collected, the highest daily rainfall data for various years was extracted and broken down to smaller duration. By applying a statistical technique known as maximum likelihood estimation, the GEV distribution was fitted to the annual maximum rainfall data. The fitted process determined the critical GEV distribution parameters, such as ϵ , σ , and ξ , that best explained the extreme rainfall occurrences found in the sample data.

Using the estimated GEV values, rainfall intensities were calculated for different durations and return times. The return period describes the average recurrence interval of an occurrence of a particular amount. In this study, return durations of two, five, ten, twenty-five, fifty, and hundred years were used. Plotted on the x-y axis, the estimated rainfall intensities for various durations and return times are displayed in the GEV stationary IDF curves. The x-axis shows the duration of the rainfall, which is stated in time units like minutes or hours, and the y-axis shows the corresponding intensity of the rainfall, which is expressed in millimeters per hour. The IDF curves provide a summary of the relationships between rainfall intensity, duration, and return periods.

Table 8: Some Meteorological Rainfall Stations and Meteorological Regions

Meteorological Region	Meteorological Station
A₁	Axum, Mekele, Maychew
A₂	Gonder, Debre Tabor, Bahir Dar, Debre Markos, Addis Ababa ,Debrezeit, Fitcha

Table 9 :Debre Markos Station Rainfall GEV Distribution Fitted Stationary Intensity Levels (mm)

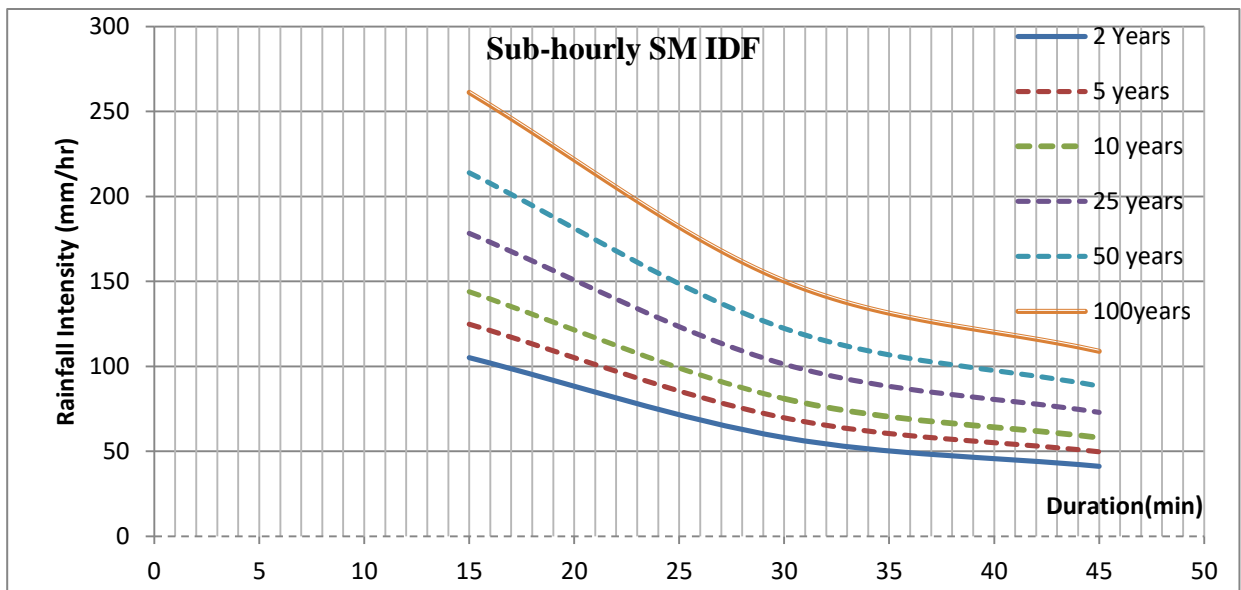
Duration(min)	Return Periods					
	2 years	5 years	10 years	25 years	50 years	100 years
15	26.28	31.20	35.98	44.57	53.48	65.30
30	29.05	34.86	40.50	50.64	61.17	75.12
45	30.89	37.30	43.52	54.69	66.30	81.67
60	32.32	39.18	45.84	57.81	70.25	86.73
120	36.17	44.28	52.15	66.29	80.98	100.43
180	38.75	47.68	56.36	71.94	88.13	109.58
Considered Dates	Return Periods					
	2 Years	5 years	10 years	25 years	50 years	100 years
1	56.708	71.42	85.71	111.37	138.05	173.37
2	59.72	71.86	81.68	96.56583	109.74	124.94
3	61.93	71.35	77.72	85.90	92.07	98.28

The quantity of rainfall exceeded or anticipated to be exceeded over a given time period and for a particular return period is known as the return levels of rainfall. Using RStudio software, a statistical examination of historical rainfall data yielded these figures. Rainfall intensity was computed using a straightforward technique after the return levels were determined.

Table 10 :Debre Markos Station Rainfall GEV Fitted Stationary Rainfall Intensity (mm/hr)

Duration(min)	Return Periods					
	2 years	5 years	10 years	25 years	50 years	100 years
15	105.12	124.8	143.92	178.28	213.92	261.2
30	58.1	69.72	81	101.28	122.34	150.24
45	41.19	49.73	58.03	72.92	88.4	108.89
60	32.32	39.18	45.84	57.81	70.25	86.73
120	18.09	22.14	26.08	33.15	40.49	50.22

180	12.92	15.89	18.79	23.98	29.38	36.52
Considered Dates	Return Periods					
	2 years	5 years	10 years	25 years	50 years	100 years
1	2.36	2.98	3.57	4.64	5.75	7.22
2	1.24	1.50	1.70	2.01	2.29	2.60
3	0.86	0.99	1.08	1.19	1.28	1.37



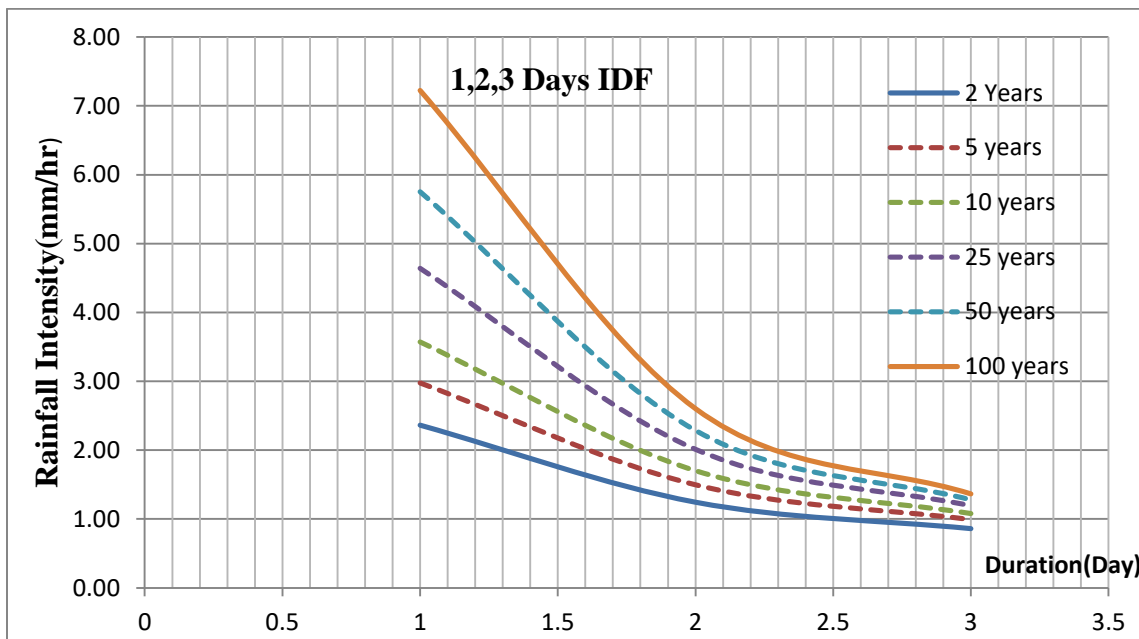
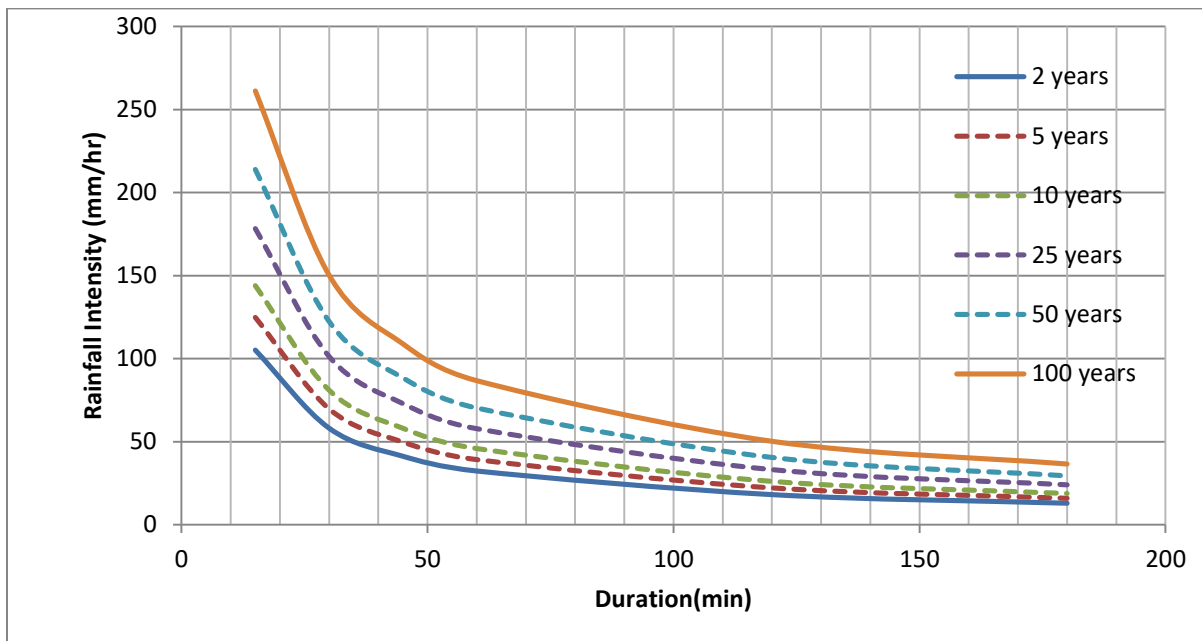


Figure 7: Debre Markos Station Rainfall Stationary Model Different Types of IDF Curves

It is important to realize that creating non-stationary IDF curves may be more difficult than creating stationary IDF curves due to the additional complexity of trend analysis and parameter

determination. Furthermore, it involved the identification of trustworthy trends and the choice of suitable trend research methodologies, which were important phases in this process.

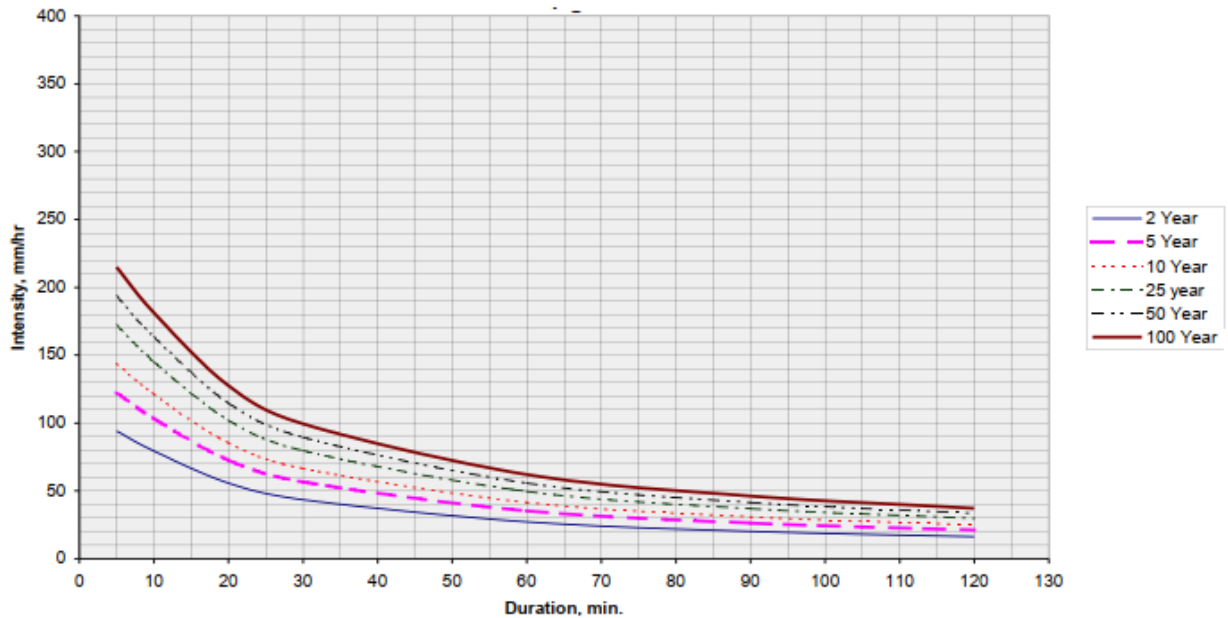


Figure 8: ERA Rainfall Region A2 and A3 IDF Curves

Table 11: Bahir Dar Airport Station Rainfall GEV Fitted Stationary Return Levels (mm)

Duration(min)	Return Periods					
	2 Years	5 years	10 years	25 years	50 years	100years
15	58.95	64.22	70.10	75.36	80.99	86.14
30	62.62	70.64	76.83	85.36	93.11	98.35
45	66.91	74.39	82.77	89.46	97.29	105.59
60	69.60	79.42	84.94	94.75	100.64	110.98
120	73.88	85.57	90.46	96.57	105.62	112.07
180	75.55	90.76	98.89	99.19	108.33	115.85
Considered Dates	Return Periods					
	2 Years	5 years	10 years	25 years	50 years	100 years
1	98.28	101.69	108.13	113.56	118.25	120.17
2	100.47	104.00	101.7375	103.3552	110.6	117.2079

3	105.13	107.98	115.13	117.16	120.27	122.27
---	--------	--------	--------	--------	--------	--------

Table 12: Bahir Dar Airport Station Rainfall GEV Fitted Stationary Rainfall Intensity (mm/hr)

Duration(min)	Return Periods					
	2 Years	5 years	10 years	25 years	50 years	100years
15	235.78	256.88	280.39	301.46	323.95	344.55
30	125.25	141.28	153.66	170.71	186.22	196.70
45	89.22	99.19	110.36	119.28	129.73	140.79
60	69.60	79.42	84.94	94.75	100.64	110.98
120	36.94	42.79	45.23	48.29	52.81	56.03
180	25.18	30.26	32.96	33.07	36.11	38.62
Considered Dates	Return Periods					
	2 Years	5 years	10 years	25 years	50 years	100years
1	4.10	4.24	4.51	4.73	4.93	5.01
2	2.10	2.11	2.12	2.15	2.30	2.44
3	1.46	1.50	1.60	1.63	1.67	1.70

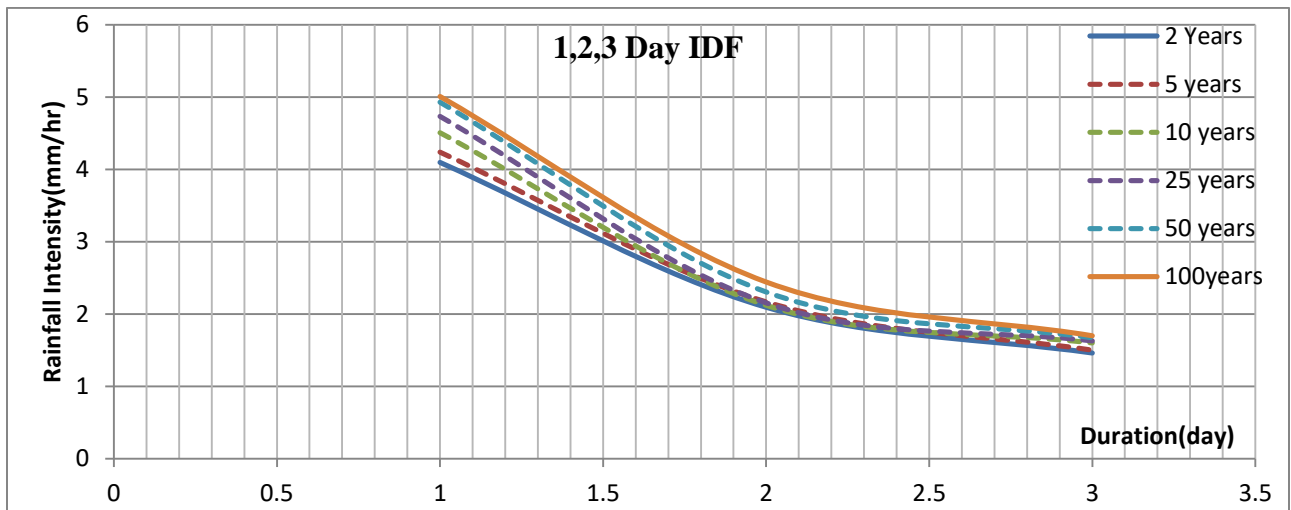
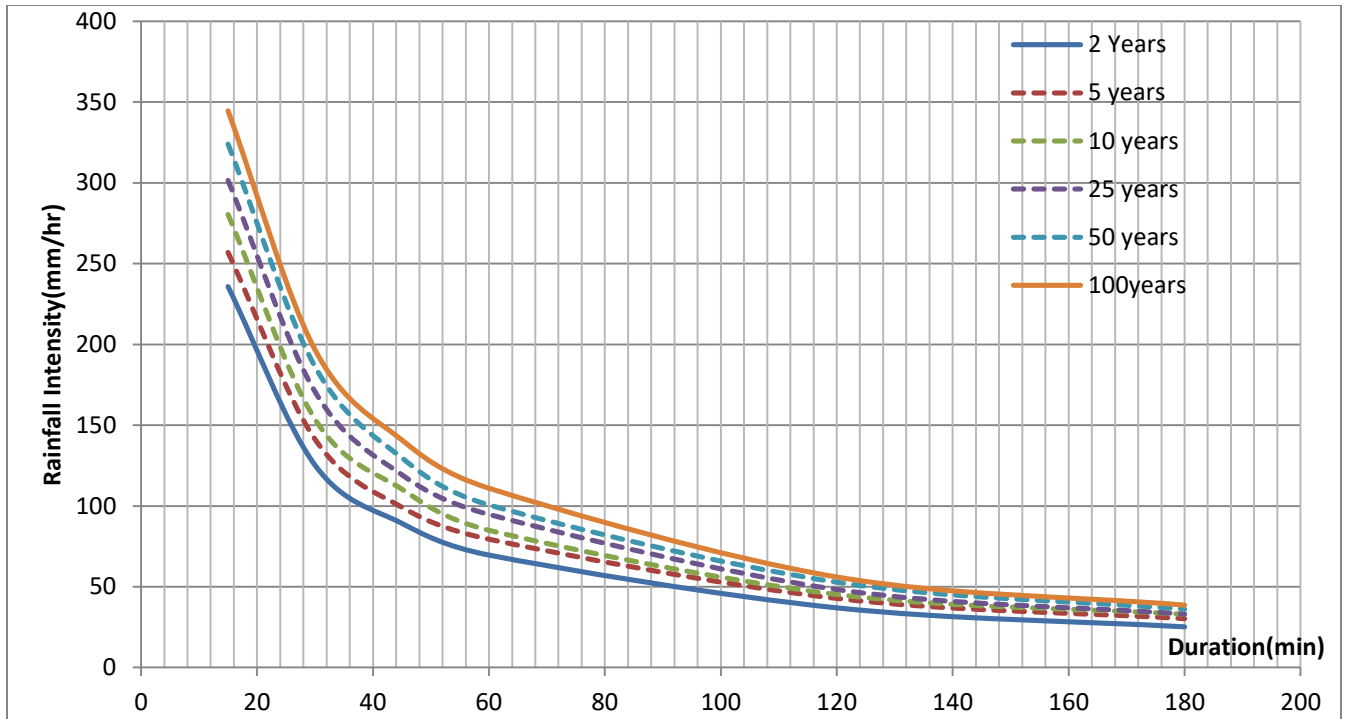


Figure 9: Bahir Dar Airport Station Rainfall GEV Fitted Stationary Model IDF Curves

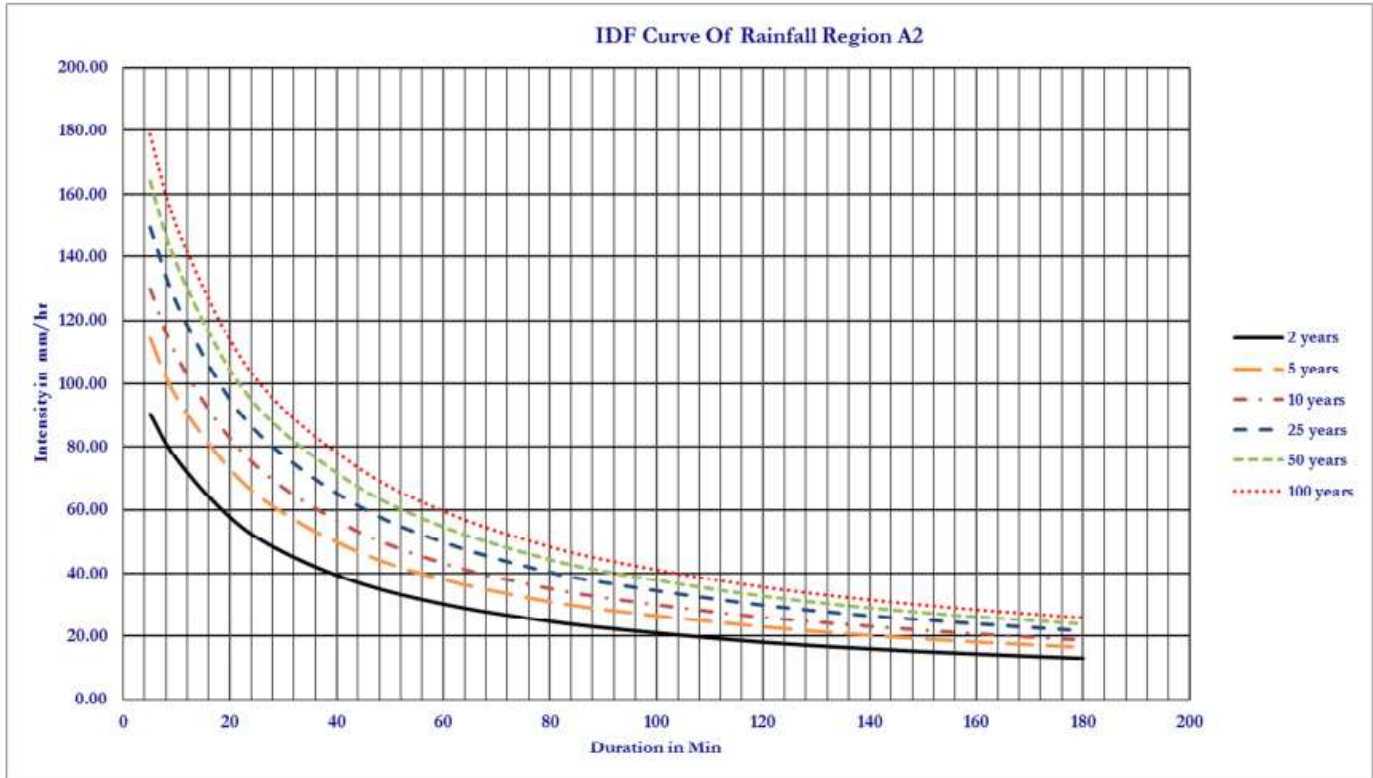


Figure 10: ERA Rainfall Region A2 IDF Curves

Table 13: Meshenti Station Rainfall GEV Distribution Fitted Stationary Return Levels (mm)

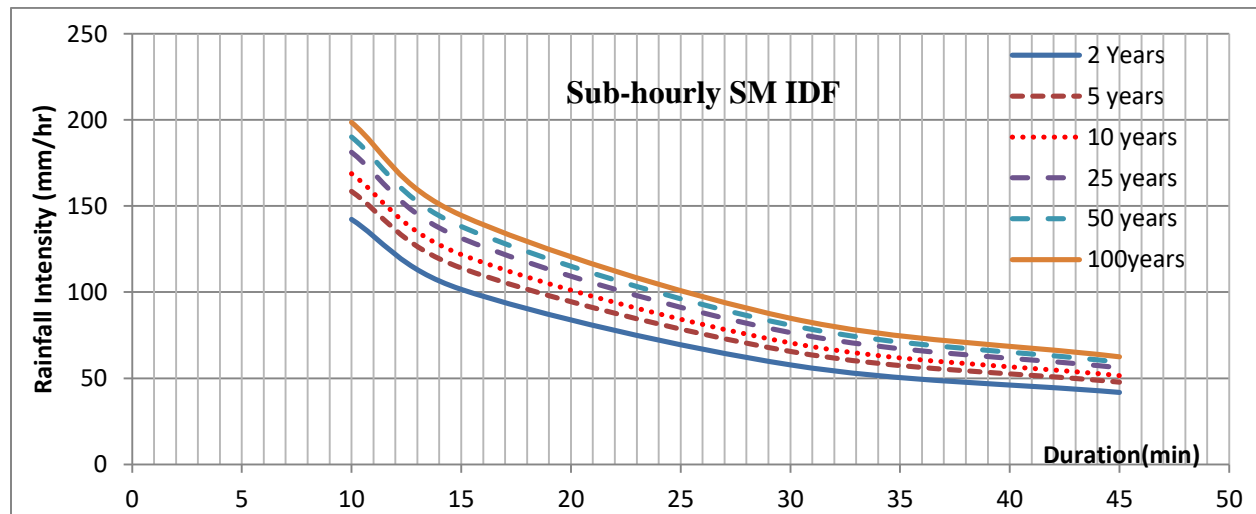
Duration (min)	Return Periods					
	2 Years	5 years	10 years	25 years	50 years	100years
10	23.71	26.42	28.13	30.20	31.68	33.1
15	25.40	28.50	30.46	32.84	34.53	36.15
30	28.89	32.79	35.26	38.25	40.38	42.42
45	31.33	35.80	38.63	42.05	44.50	46.83
60	33.27	38.20	41.31	45.08	47.76	50.33
120	38.80	45.00	48.92	53.67	57.06	60.30
180	45.77	53.58	58.52	64.50	68.77	72.85

While rainfall intensity decreases with increasing duration and increases with increasing return period, return levels or intensity levels increase as both the duration and return periods grow.

Higher rainfall intensities and smaller rainfall volumes are characteristic of these shorter timeframes.

Table 14 :Meshenti Station Rainfall GEV Distribution Fitted Stationary Rainfall Intensity (mm/hr)

Duration(min)	Return Periods					
	2 Years	5 years	10 years	25 years	50 years	100years
10	142.24	158.50	168.77	181.21	190.08	198.57
15	101.61	114.00	121.85	131.35	138.11	144.60
30	57.77	65.60	70.52	76.51	80.76	84.85
45	41.77	47.73	51.50	56.07	59.32	62.44
60	33.27	38.20	41.30	45.08	47.76	50.33
120	19.40	22.50	24.46	26.84	28.53	30.15
180	11.44	13.40	14.63	16.13	17.19	18.21



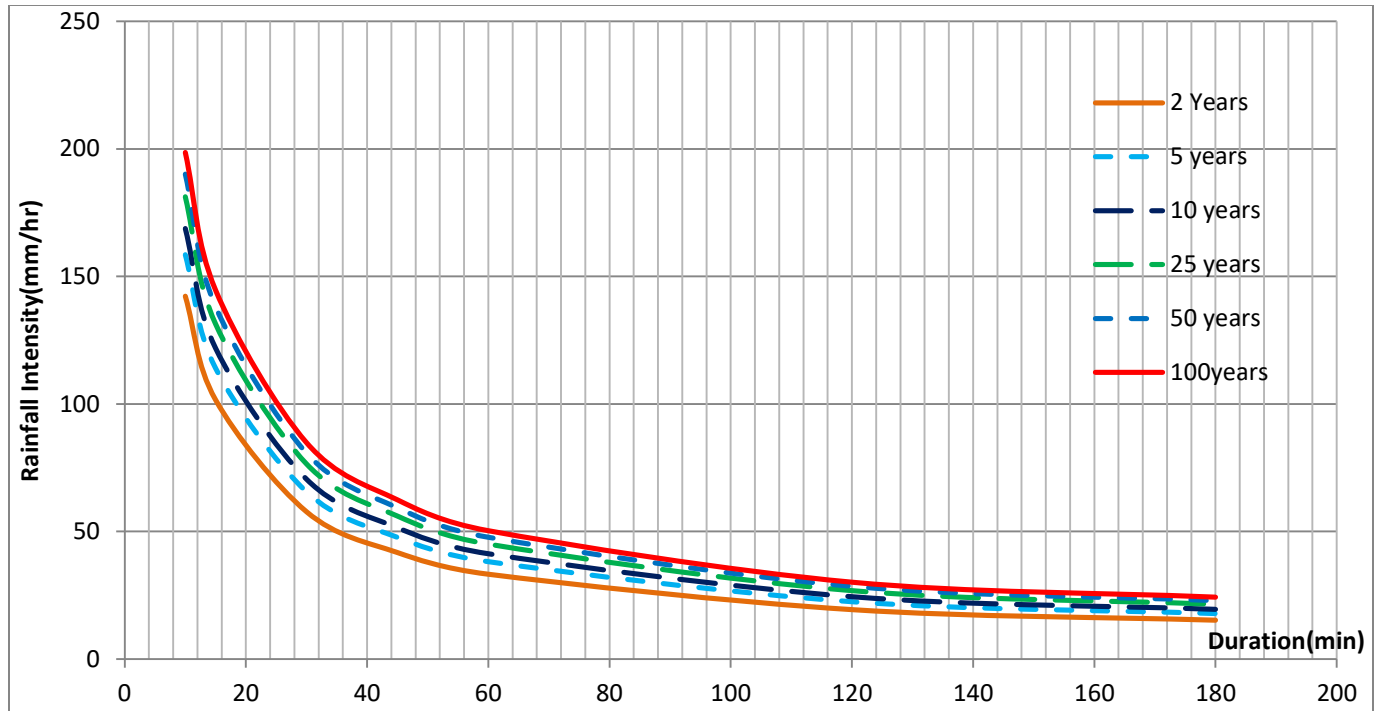


Figure 11: Meshenti Station Rainfall Stationary IDF Curves

The IDF curves approach the origin and get larger as return periods get longer and smaller as duration increases. The graph illustrates this; the IDF curve for 100 years is at the top and the IDF curve for a 2-year return period is at the bottom.

Hourly stationary models have intensity levels that are higher than sub-hourly values; the values also rise with an increase in duration and return period. Sub-hourly stationary models, on the other hand, have significantly greater intensity values than hourly stationary models. As the durations rise, the curves approach the x-axis quite closely.

The hourly IDF curves are close to the origin and divergent from each other when compared to sub-hourly IDF curves.

Table 15: Tisabay Station Rainfall GEV Fitted Stationary Return Levels (mm)

Duration(minute)	Return Periods					
	2years	5years	10years	25 years	50years	100years
10	20.32	23.46	25.11	26.82	27.86	28.73
15	21.81	25.39	27.29	29.24	30.43	31.42

30	24.88	29.40	31.78	34.24	35.74	36.99
45	27.03	32.20	34.93	37.75	39.46	40.90
60	28.75	34.44	37.44	40.54	42.42	44.01
120	33.62	40.79	44.57	48.48	50.85	52.85
180	37.04	45.24	49.57	54.04	56.76	59.05
Considered Dates	2years	5years	10years	25 years	50years	100years
1	54.07	70.49	79.15	88.09	93.53	98.10
2	55.03	67.19	72.94	78.31	81.28	83.58
3	22.00	89.00	133.00	189.00	230.00	271.00

Table 16: Tisabay Station Rainfall GEV Fitted Stationary Rainfall Intensity (mm/hr)

Duration(minute)	Return Periods					
	2years	5years	10years	25 years	50years	100years
10	121.94	140.74	150.66	160.90	167.13	172.37
15	87.24	101.58	109.14	116.95	121.70	125.69
30	49.76	58.79	63.56	68.48	71.47	73.98
45	36.04	42.94	46.57	50.33	52.61	54.53
60	28.75	34.44	37.44	40.54	42.42	44.01
120	16.81	20.39	22.29	24.24	25.43	26.42
180	12.35	15.08	16.52	18.01	18.92	19.68
Considered Dates	2years	5years	10years	25 years	50years	100years
1	2.3	2.9	3.3	3.7	3.9	4.1
2	1.1	1.4	1.5	1.6	1.7	1.7
3	0.3	1.2	1.8	2.6	3.2	3.8

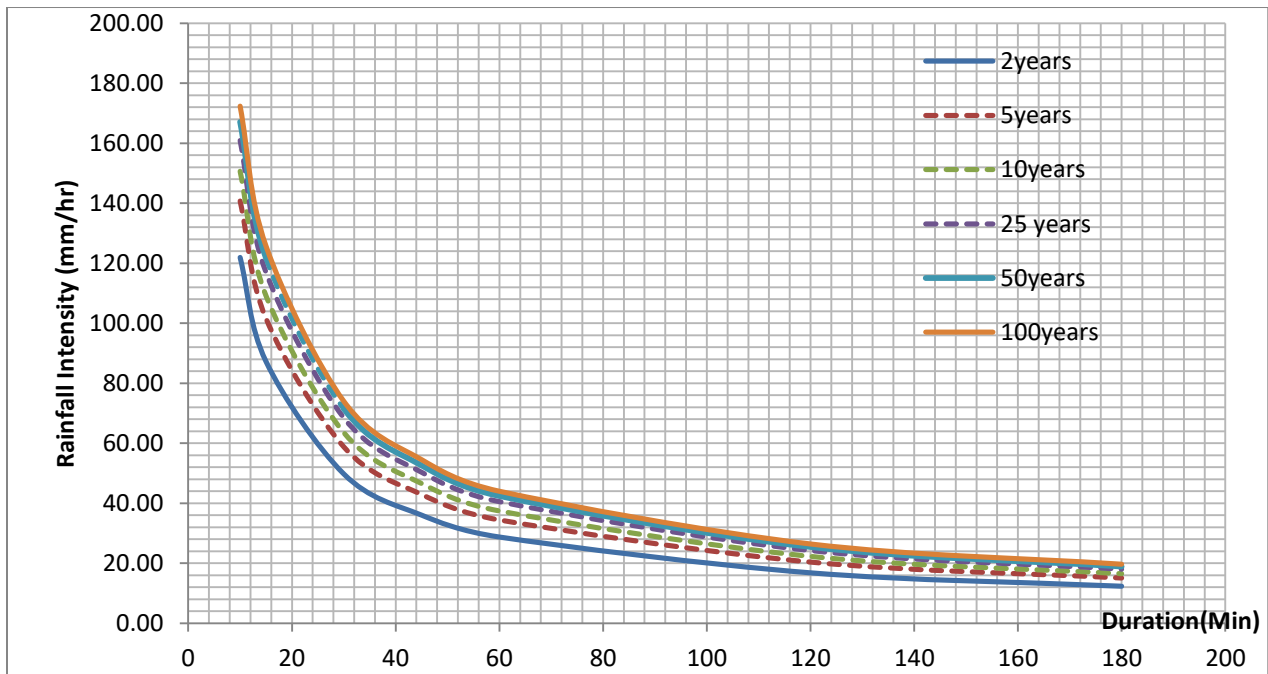
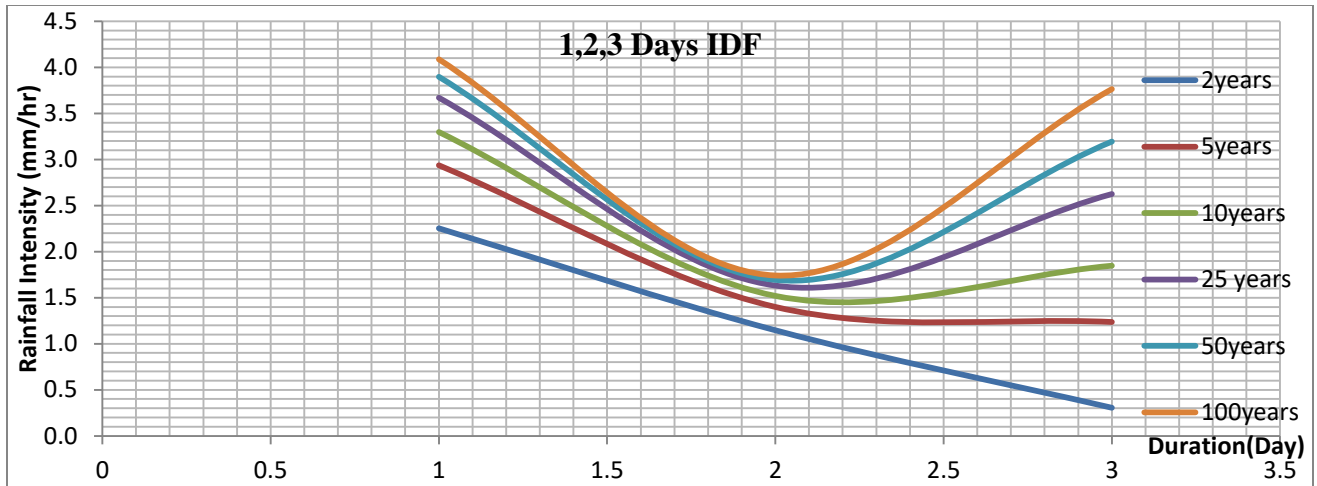


Figure 12: Tisabay Station Rainfall GEV Distribution fitted Stationary IDF Curves

4.11 Comparing ERA Regional and Stationary Model Rainfall Intensities

Table 17: ERA Rainfall Intensity for Region A2 and A3 (mm/hr)

Duration(min)	Return Period					
	2 years	5 years	10 years	25 years	50 years	100 years
15	67	110	140	170	190	230
30	43	57	75	89	100	100
45	35	45	50	62	75	90

60	28	35	40	50	57	62
120	18	20	23	30	37	40

Table 18: Debre Markos Station Rainfall Stationary Model Rainfall Intensity (mm/hr)

Duration(min)	Return Periods					
	2 years	5 years	10 years	25 years	50 years	100 years
15	105.12	124.8	143.92	178.28	213.92	261.2
30	58.1	69.72	81	101.28	122.34	150.24
45	41.19	49.73	58.03	72.92	88.4	108.89
60	32.32	39.18	45.84	57.81	70.25	86.73
120	18.09	22.14	26.08	33.15	40.49	50.22
180	12.92	15.89	18.79	23.98	29.38	36.52

Table 19: Comparison of Table 17 and Table 18 ERA and Debre Markos Station Rainfall Stationary Model Rainfall Intensities

15 Minutes Duration			
Rerun Period	Stationary Model Intensity(mm/hr)	ERA Intensity(mm/hr)	Difference
2	105.12	67	38.12
5	124.8	110	14.8
10	143.92	140	3.92
25	178.28	170	8.28
50	213.92	190	23.92
100	261.2	230	31.2
30 Minutes duration			
Rerun Period	Stationary Model	ERA	Difference

	Intensity(mm/hr)	Intensity(mm/hr)	
2	58.1	43	15.1
5	69.72	57	12.72
10	81	75	6
25	101.28	89	12.28
50	122.34	100	22.34
100	150.24	100	50.24
45 Minutes duration			
Rerun Period	Stationary Model Intensity(mm/hr)	ERA Intensity(mm/hr)	Difference
2	41.19	35	6.19
5	49.73	45	4.733
10	58.03	50	8.03
25	72.92	62	10.92
50	88.4	75	13.4
100	108.89	90	19.90
60 Minutes duration			
Rerun Period	Stationary Model Intensity(mm/hr)	ERA Intensity(mm/hr)	Difference
2	32.32	28	4.32
5	39.18	35	4.18

4.12 Validation for Rainfall

The process of comparing observed and anticipated rainfall amounts is known as rainfall value validation. Depending on the particular situation, the data that is available, and the goal of the rainfall value predictions, there are several approaches to validation.

The validation procedure requires specialized knowledge and comprehension in order to express the results and analyze the overall reliability of rainfall intensity estimates.

Table 20: Comparison of Observed and Disaggregated Rainfall

15 Minute				30 Minute		
Year	Observed	Disaggregated	Difference	Observed	Disaggregated	Difference
2019	18.8	27.18	8.38	24	30.11	6.11
2021	15.3	28.99	13.69	26.6	32.25	5.65
2022	16	22.6	6.6	17	24.7	7.7

45minute			60 minute		
Observed	Disaggregated	Difference	Observed	Disaggregated	Difference
31.8	32.07	0.27	33.7	33.9	0.2
30.4	34.42	4.02	32.5	36.09	3.59
18.4	26.1	7.7	19.6	27.18	7.58

The two tables above showed that there are positive differences within a good range between the disaggregated and observed rainfall storms. This demonstrated that every estimate is accurate in relation to the actual rainfall records. This indicates that there is no chance of extreme events and that the projected total rainfall levels are not underestimated. Thus, this is a sign of how well the model's simulation procedures of past data have worked.

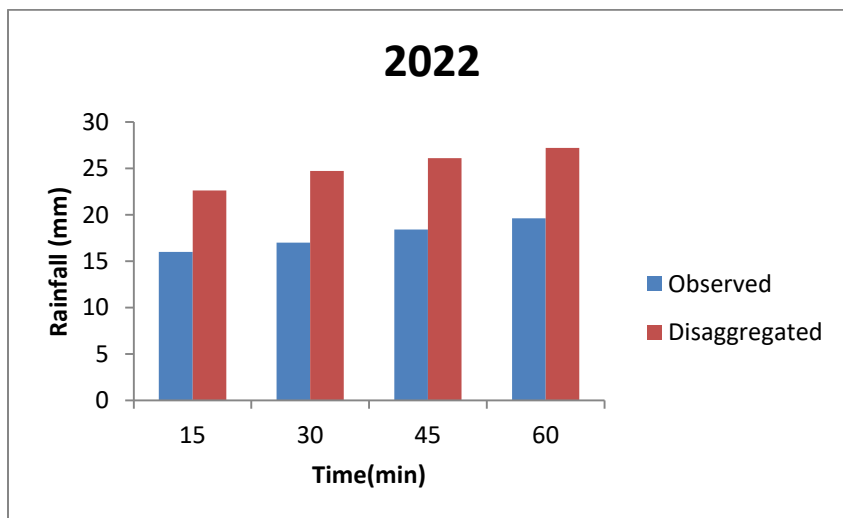
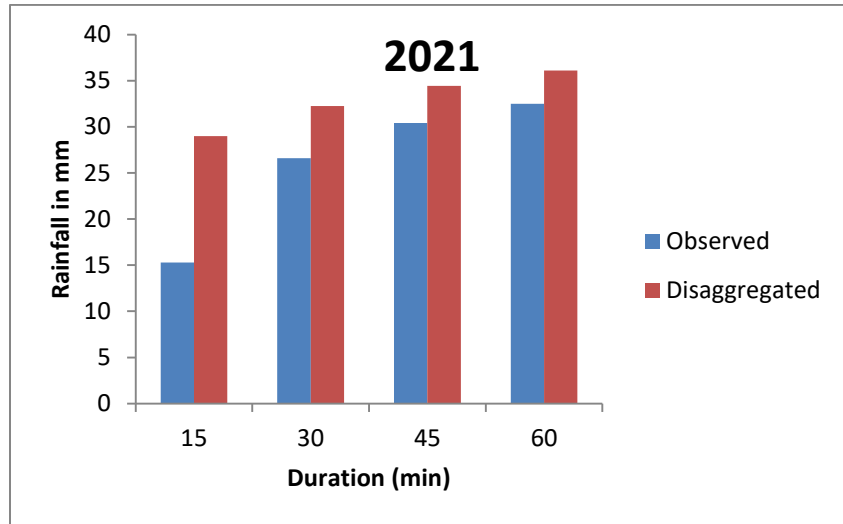
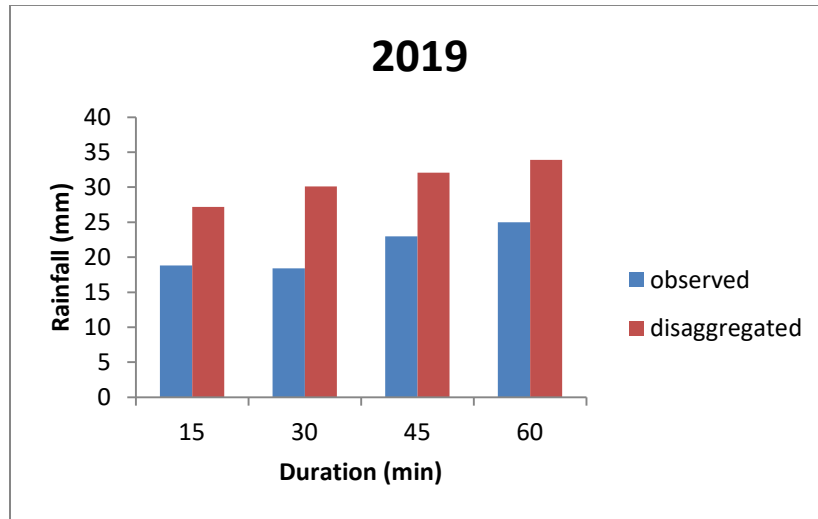


Figure 13: Validation for Rainfall Depth

The disaggregated rainfall values are slightly higher than the observed levels, as the histogram plots clearly demonstrated. For Merawi Town, a superior outcome was obtained by comparing the daily rainfall data from the observed and disaggregated model simulated rainfall data over the validation period. The figures demonstrate that the outcomes of the model simulation closely match the observed results, which is positive evidence of our work.

4.13 Validation for Rainfall Intensity

Validation for intensity, like validation for rainfall values, involves comparing measured and forecasted rainfall intensities with rainfall intensities derived from observed rainfall. Several approaches to validation can be taken depending on the particular situation, the data at hand, and the intended use of rainfall intensity estimations. In the validation procedure, specific expertise and comprehension are essential for expressing the outcomes and analyzing the overall dependability of rainfall intensity estimates.

Table 21: Exceedance Probability and Return Periods of Observed Rainfall

15 Minute			(m-0.5)/n	30 Minute						
Year	Rainfall	Rank	Probability of exceedance	Return Period	I(mm/hr)	Rainfall	Rank	Probability of exceedance	Return Period	I(mm/hr)
2019	18.8	1	16.67	6	75.2	24	2	50	2	48
2021	15.3	3	83.33	1.2	61.2	26.6	1	16.67	6	53.21
2022	16	2	50	2	64	17	3	83.33	1.2	34

45Minutes					
Year	Rainfall	Rank	Probability of exceedance	Return period	I(mm/hr)
2019	18.4	3	83.33	1.2	24.5
2021	31.81	1	16.67	6	42.41
2022	30.4	2	50	2	40.5

60 Minutes					
Year	Rainfall	Rank	Probability of exceedance	Return period	I(mm/hr)
2019	33.7	1	16.67	6	33.7
2021	32.5	2	50	2	32.5
2022	19.6	3	83.33	1.2	19.6

Table 22: Rainfall Intensity (mm/hr) Derived from Observed Rainfall Using Standard Equation

Duration(minutes)	1.2 Years Return Period	2 Years Return Period	6 Years Return Period
15	61.2	64	75.2
30	34	48	53.2
45	24.53	40.53	42.40
60	19.6	32.5	33.7

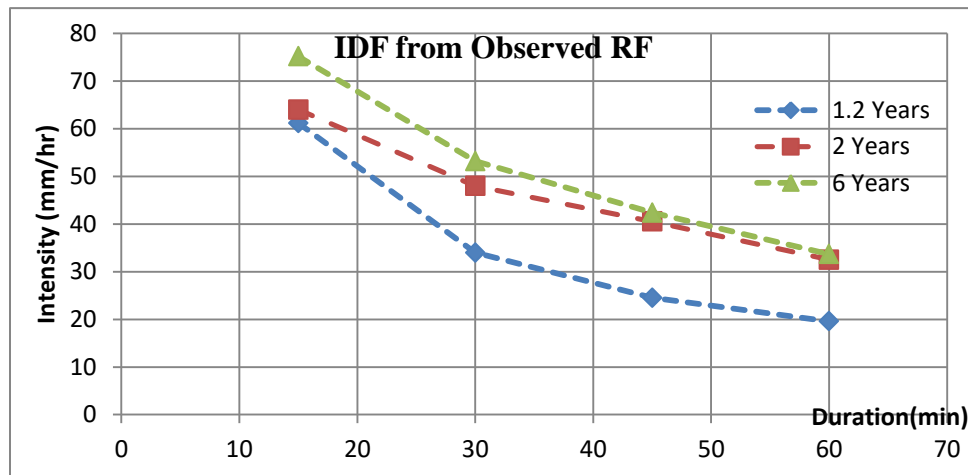


Figure 14: IDF Curves from Observed Rainfall Data Using Standard Equation

Table 23: GEV Distribution Fitted Disaggregated Intensity Levels (mm)

Duration(min)	1.2 Years Return period	2 Years Return period	6 Years Return period
15	23.78	26.41	32.91
30	26.08	29.20	37.21
45	27.63	31.06	39.89
60	28.82	32.50	41.96

Table 24: GEV Distribution Fitted Stationary Disaggregated Rainfall Intensity (mm/hr)

Duration(min)	1.2 Years Return period	2 Years Return period	6 Years Return period
15	95.12	105.64	131.64
30	52.16	58.4	74.42
45	36.84	41.41	53.19
60	28.82	32.5	41.96

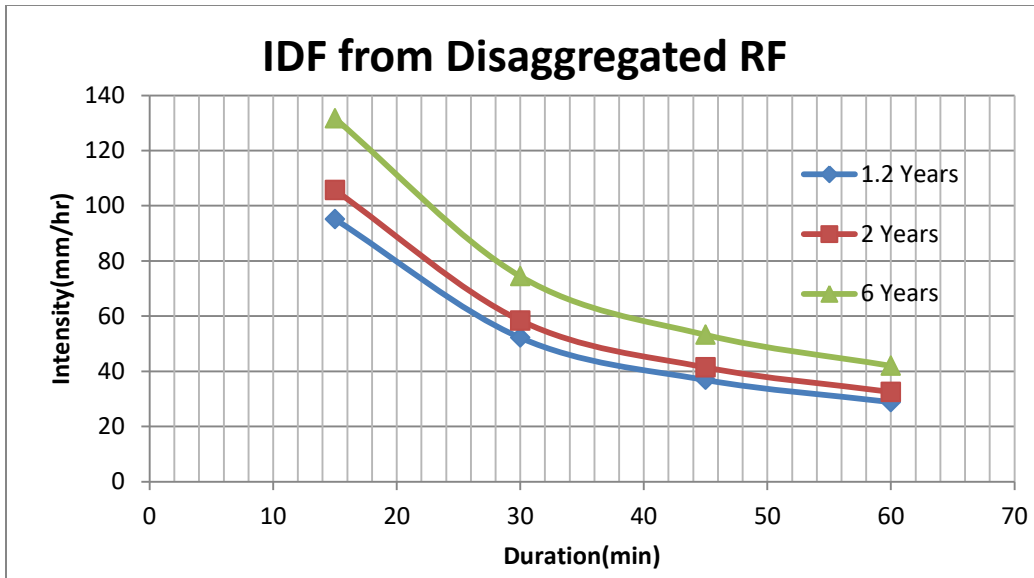
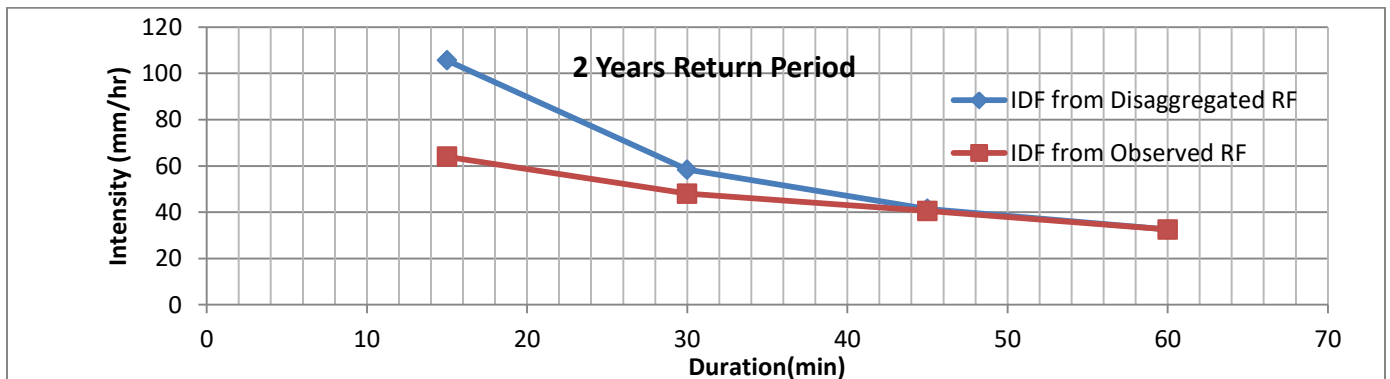
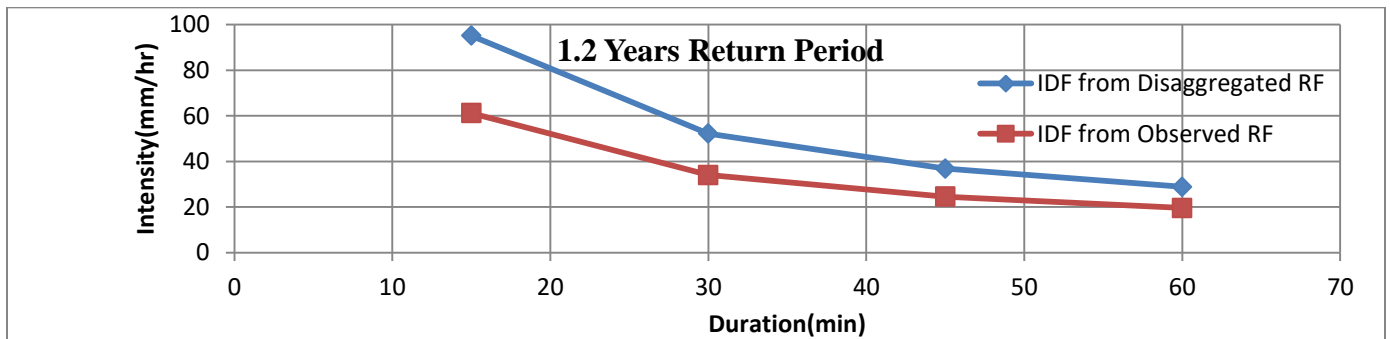


Figure 15: IDF Curves from Disaggregated Rainfall Data

The above tables and IDF plots at 1.2 years return period show that, at 15 minutes of observed rainfall, the intensity was 61.2 mm/hr. At the same return period and duration, the stationary method produced an intensity of 95.12 mm/hr. This indicates a positive difference and shows that the stationary method did not underestimate the intensity of the rainfall compared to the benchmark of observed rainfall.



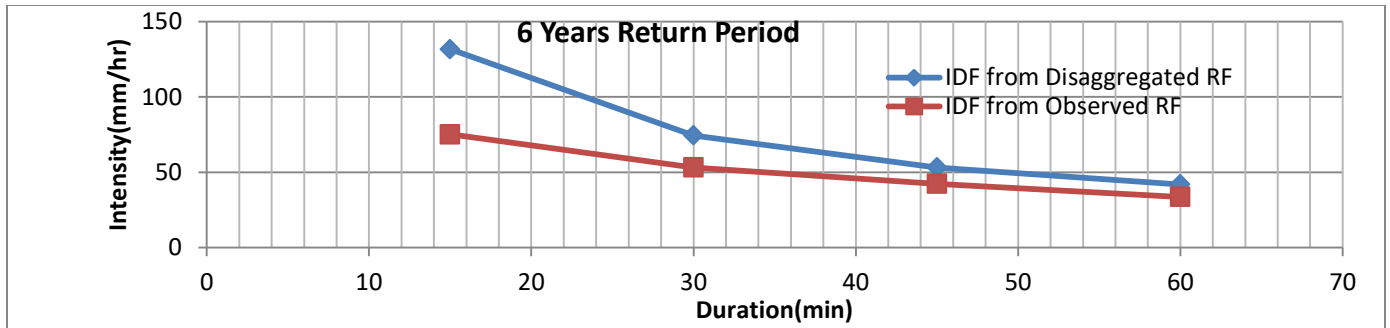


Figure 16: Observed and Disaggregated IDF Curves on the Same Normal Paper

To enhance understanding, the model historical rainfall intensity for the same station was shown versus durations with corresponding return periods, and the sample distribution of observed rainfall intensity was also plotted. Similar trends may be seen in the rainfall intensity distribution of the historical model sample data that has been disaggregated and the observed sample data. This shows that the model simulates better results and has a very excellent indexes anticipated value agreement with real available data, indicating that the simulation quality of the model is good.

CHAPTER 5: CONCLUSION

A crucial job in hydrology for the prediction of extreme rainfall occurrences is the creation of intensity duration frequency curves. Stationary models, which assume certain distribution characteristics stay constant over time, have been used historically to create IDF curves. The annual maximum daily rainfall of each station as well as automatically collected annual maximum sub-hourly (minute) rainfall data was utilized to create intensity duration frequency curves for Merawi Town using the generalized extreme value distribution stationary approach.

The yearly maximum daily rainfall data from the station are verified using several methods and confirmed to be independent, stationary, and homogeneous. In addition to these data checks, the rainfall data was subjected to trend test analysis using the Mann-Kendall technique, but no trend was seen in any of the stations. The model fitting procedures were examined, and the distribution parameter and return levels were estimated, using the R-Studio software. The generalized extreme value estimator approach was employed to forecast the distribution parameters, and the parameters were executed using RStudio, an integrated R software program.

When IDF curves were plotted for stationary model intensities, it was found that the durations were investigated in two portions. This resulted from the precipitation intensities' peculiar behavior over the course of two durations [15 minutes, 60 minutes] and [1 hour, 24 hours], where shorter durations saw higher rainfall intensity values than longer ones.

In practice, longer return periods yielded higher values than shorter return periods when computing rainfall intensity. For instance, a 15-minute rainstorm stationary model with a 25-year return period produced an intensity of 178.28 mm/hr, while a 15-minute rainstorm with a 100-year return period produced 261.2 mm/hr of rainfall.

As a result, the stationary IDF models approximated peak floods based on the severity of the rainfall, especially for shorter durations. It was confirmed that there was a noticeable increase in the variation in rainfall intensities between stationary elements for times between 10 and 60 minutes. On the other hand, the intensity values of rainfall declined as the durations increased, suggesting that shorter events grew more intense over time, whereas longer events did not. For the purpose of designing various structures, analysis of these storms should concentrate on shorter durations since shorter storms are producing higher intensities and showing signs of a

greater difference in the extreme values, which could increase the risk of flooding and cause the failure of hydraulic and hydrologic infrastructures.

In summary, the research demonstrates the significance and practical application of the GEV distribution stationary model in understanding extraordinary occurrences. Through the provision of analytical information on the behavior of catastrophic occurrences, this model aids in improving risk management and decision making across the Town.

CHAPTER 6: RECOMMENDATION

- ❖ Engaging with local authorities, engineers, and water resource managers in Merawi Town from the beginning to final work will help to get better findings and recommendations of the IDF curve development for study the area
- ❖ All towns in Ethiopia should have complete and sufficient historical rainfall data records together with automatically recorded rainfall for longer years of record , either at Universities or at the relevant regional and country level offices
- ❖ An R statistical programming environment should be used to implement the GEV stationary method for developing the IDF curves
- ❖ It is advised to analyze the implications of using different IDF curve estimation methods on the design and planning of water infrastructure systems in Merawi Town.
- ❖ Non-stationary IDF modeling should be taken into consideration when developing intensity-duration-frequency curves for various towns and cities.

REFERENCES

- WMO, W. M. (1978). *World Meteorologica Manual on intensity-duration-frequency (IDF) curves*. Geneva, Switzerland: WMO.
- Climate Change and Rainfall Intensity–Duration–Frequency Curves verview of Science and Guidelines for Adaptation. (2016). *ASCE*, 18.
- (2018). *North Mecha Woreda and Merawi Town 2019 to 2030 West Gojjam Zone, Amhara National Regional State*.
- Andre Schardong, S. P. (2020). Web-Based Tool for the Development of Intensity Duration Frequency Curves under Changing Climate at Gauged and Ungauged Locations. *Water*, 31.
- Asi G. Sam, I. L. (2023). Modeling Rainfall Intensity-Duration-Frequency(IDF) and Establishing Climate Change Existence in Uyo-Nigeria Using Non-Stationary Approach. *Journal of Water Resource and Protecti*, 8.
- Asikoglu, O. L. (2017). Outlier Detection in Extreme Value Series. *Journal of Multidisciplinary Engineering Science and Technology*, 5.
- Berger., G. C. (2021). *Statistical Inference*. Newdelhi.
- Casella, G. &. (2002). *Statistical inference (2nd ed.)*. *Duxbury Press*, 13.
- Chaw, V. T. (1988). *Applied Hydrology*. California: McGRAW-Hill international Edition.
- Chow, V. T. (1988). *Applied Hydrology* . New York : Mc Gra-Hill.
- Christian Charron, T. B. (2018). Non-stationary intensity-duration-frequency curves integrating information concerning teleconnections and climate change. *Inernational Journal of Climatology* , 18.
- Coles, S. (2001). *An Introduction to Statistical Modeling of Extreme Values*. *Springer*, 17.
- Conover, W. J. (1981). Rank transformations as a bridge between parametric and nonparametric statistics. *The American Statistician*, 35(3), 124-129.
- Daniele Feitoza Silva, I. P. (2021). Introducing Non-Stationarity Into the Development of Intensity-Duration-Frequency Curves under a Changing Climate. *Water* , 21.

- Daniele Feitoza Silva, S. P. (2021). Introducing Non-Stationarity Into the Development of Intensity-Duration-Frequency Curves under a. *Water*, 22.
- Elizabeth, M. (1994). Hydrology in Practice. In M. Elizabeth, *Hydrology in Practice* (p. 628).
Tottenham: Chapman & Hall.
- Esri.com. (2023, December 29). *ArcGIS Pro*. Retrieved December 29, 2024, from ArcGIS Pro:
<https://www.esri.com/en-us/arcgis/products/arcgis-pro/overview>
- Haktanir, T. (2014). Trend, independence, stationarity, and homogeneity tests on maximum rainfall series of standard durations recorded in Turkey. *Journal of Hydrologic Engineering*, 38.
- Han Jiqina, F. (2023). Application of MK trend and test of Sen's slope estimator to measure impact of climate change on the adoption of conservation agriculture in Ethiopia. *Journal of Water and Climate Change*, 12.
- Hargreaves, G. L. (2014). Assessing the quality of weather data and its relevance to horticultural science. *HortScience*, 47.
- Henson, R. &. (2019). Rainfall: Weather Past, Present and Future. *Journal of Hydrology*, 20.
- Hershey, J. R. (1955). Frequency analysis of rainfall. *Hydrology*, 1-10.
- Ify L. Nwaogazie, M. G. (2023). Modeling Rainfall Intensity-Duration-Frequency and Establishing Climate Change Existence in Uyo-Nigeria Using Non-Stationary Approach. *Journal of Water Resource and Protection*, 21.
- Ikebude, C. (2023). Modeling Rainfall Intensity-Duration-Frequency(IDF) and Establishing Climate Change Existence in Uyo-Nigeria Using Non-Stationary Approach. *Journal of Water Resource and Protection*, 21.
- IPCC. (AR5). *provide comprehensive information on observed and projected changes in rainfall patterns due to climate change*. New York: IPCC.
- K.Subramanya. (2005). *Engineering Hydrology*. New Delhi : Tata McGraw-Hill.
- Kasiviswanathan, T. Z. (2023). A Bayesian modelling approach for assessing non A Bayesian modelling approach for assessing non changing climate. *changing climate*, 2020.

- Katz, L. C. (2014). Non-stationary extreme value analysis in a changing climate. *Climatic Change*, 17.
- Lalani Jayaweera, C. W. (2023). Non-stationarity in extreme rainfalls across Australia. *Journal of Hydrology*, 15.
- Lewoyehu, M. (2021). Evaluation of Drinking Water Quality in Rural Area of Amhara Region, Ethiopia: The Case of Mecha District. *Journal of Chemistry*, 11.
- Linyin Cheng, A. A. (2014). Non-stationary extreme value analysis in a changing climate. *Climatic Change*, 17.
- M. Carmen Casas-Castillo, X. N.-S. (2016). A study of the scaling properties of rainfall in Spain and its appropriateness to generate intensity-duration-frequency curves from daily records. *INTERNATIONAL JOURNAL OF CLIMATOLOGY*, 11.
- Masi G. Sam, I. L. (2023). Modeling Rainfall Intensity-Duration-Frequency (IDF) and Establishing Climate Change Existence in Uyo-Nigeria Using Non-Stationary Approach. *Scientific Research*, 21.
- Microsoft. (2023, December 29). *Microsoft*. Retrieved December 29, 2023, from Microsoft Excel Official Website: <https://www.microsoft.com/en-us/microsoft-365/excel>
- Mohammed S. Shamkhi. (2022). Deriving rainfall intensity–duration–frequency (IDF) testing the best distribution using EasyFit software 5.5 for Kut city, Iraq. *De Gruyter*, 1-10.
- Mohita Anand Sharma, J. B. (2010). Use of Probability Distribution in Rainfall Analysis. *New York Science Journal*, 10.
- Mohita Anand Sharma, J. B. (2010). Use of Probability Distribution in Rainfall Analysis. *New York Science Journal*, 10.
- Petitjean, M. (1999). On the Root Mean Square quantitative chirality and quantitative symmetry measures. *Journal of Mathematical Physics*, 9.
- Posit. (2023, December Friday). *Posit*. Retrieved December Friday, 2023, from RStudio website: <https://docs.rstudio.com/>
- Prerana Chitrakar a, A. S. (2023). Regional distribution of intensity–duration–frequency (IDF) relationships in Sultanate of Oman. *Journal of King Saud University – Science*, 14.

- Raghunath. (2006). Hydrology principles analysis design. In Raghunath, *Hydrology principles analysis design* (p. 477). Newdelhi: New Age International puplisher.
- Raúl Rodríguez-Solà, a. M.-C. (2017). A study of the scaling properties of rainfall in spain and its appropriateness to generate intensity-duration-frequency urves from daily records. *INTERNATIONAL JOURNAL OF CLIMATOLOGY*, 11.
- Sam, M. N. (2023). Modeling Rainfall Intensity-Duration-Frequency Modeling Rainfall Intensity-Duration-Frequency Non-Stationary Approach. *Journal of Water Resource and Protection*, 20.
- Sattari, A. R.-J. (2017). Assessment of different methods for estimation of missing data in precipitation studies. *Hydrology Research*, 13.
- Shamkhi, M. K. (2022). Deriving rainfall intensity–duration–frequency (IDF) curves and testing the best distribution using EasyFit software 5.5 for Kut city, Iraq. *DE GRUYTER*, 10.
- Silva, D. F. (2021). Introducing Non-Stationarity Into the Development of Intensity-Duration-Frequency Curves under a Changing Climate. *Water*, 22.
- Simeneh Melesse, G. (2016). Development of Intensity Duration Frequency(IDF) Curves for Bahir Dar City from Daily Rainfall Data by Using Simple Scaling Method,Bahir Dar, Ethiopia. *Addis abeba university*, 89.
- Tanchev, L. (2014). *Dams and appurtenant Hydraulic structures* . London, UK: CPI Group (UK) Ltd.
- Tegenu, M. T. (2021). Development of Intensity Duration Frequency Curves for Wolkite Town. *International Journal on Data Science and Technology*, 9.
- Thein, S. H. (2019). Modelling of Short Duration Rainfall IDF Equation for Sagaing Region, Myanmar. *American Scientific Research Journal for Engineering, Technology, and Sciences (ASRJETS)*, 14.
- Thein, Sai Htun . (2019). Modelling of Short Duration Rainfall IDF Equation for Sagaing Region, Myanmar. *American Scientific Research Journal for Engineering, Technology, and Sciences (ASRJETS)*, 5-7.

WaterAid, E. (2018). *North Mecha Woreda and Merawi Town 2019 to 2030 West Gojjam Zone, Amhara National Regional State*. Merawi: 44.